Selective B cell depletion upon intravenous infusion of replication-incompetent anti-CD19 CAR lentivirus

Craig M. Rive[a], Eric Yung[a], Lisa Dreolini[a], Scott D. Brown[a], Christopher G. May[a], Daniel J. Woodsworth[a], Robert A. Holt [a,b,c,2]

[a] Canada's Michael Smith Genome Sciences Centre, BC Cancer, Vancouver, BC, V5Z 1L3, Canada.
[b] Department of Medical Genetics, University of British Columbia, Vancouver, BC, V6T 1Z4, Canada.
[c] Molecular Biology & Biochemistry, Simon Fraser University, Burnaby, BC, V5A 1S6, Canada.
[2] Correspondence: rholt@bcgsc.ca, Canada's Michael Smith Genome Sciences Centre, BC Cancer, Vancouver, British Columbia, Canada

Abstract

Anti-CD19 CAR-T therapy for B cell malignancies has shown clinical success, but a major limitation is the logistical complexity and high cost of manufacturing autologous cell products. If engineered for improved safety, direct infusion of viral gene transfer vectors to initiate *in vivo* CAR-T transduction, expansion and anti-tumor activity could provide an alternative, universal approach. To explore this approach we administered approximately 20 million replication-incompetent VSV-G lentiviral particles carrying an anti-CD19CAR-2A-GFP transgene comprising either an FMC63 (human) or 1D3 (murine) anti-CD19 binding domain, or a GFP-only control transgene, to wild-type C57BL/6 mice by tail vein infusion. The dynamics of immune cell subsets isolated from peripheral blood were monitored at weekly intervals. We saw emergence of a persistent CAR-transduced $CD3^+$ T cell population beginning week 3-4 that reached a maximum of 13.5 +/- 0.58% (mean +/- SD) and 7.8 +/- 0.76% of the peripheral blood $CD3^+$ T cell population in mice infused with ID3-CAR or FMC63-CAR lentivector, respectively, followed by a rapid decline in each case of the B cell content of peripheral blood. Complete B cell aplasia was apparent by week 5 and was sustained until the end of the protocol (week 8). No significant CAR positive populations were observed within other immune cell subsets or other tissues. These results indicate that direct IV infusion of conventional VSV-G pseudotyped lentiviral particles carrying a CD19 CAR transgene can transduce T cells that then fully ablate endogenous B cells in wild type mice.

Keywords: CAR-T, Immune effector cells; viral vector, gene transfer, gene therapy, leukemia, lymphoma

Introduction

Ordinarily, a cancer patient's immune system can recognize cancer cells as being altered, and mount a natural immune response. T cells are known to be the main mediators of the anti-cancer immune response but sometimes the natural T cell response is ineffective; T cells may fail to recognize tumor cells, fail to activate, or fail to sustain a response long enough to have an impact. It is possible for these limitations to be overcome by genetic engineering strategies that involve isolating a sample of a patient's T lymphocytes, genetically modifying and activating the cells *ex vivo*, and then re-administering them to the same patient. The genetic modification step involves introducing into the T cells an extra gene that carries instructions for a new antigen receptor that may be, for example, a recombinant alpha-beta T cell receptor (αβTCR) or a Chimeric Antigen Receptor (CAR). Much of the growing interest in genetically engineered IECs as a new class of therapeutic is

driven by the impressive results CAR-T therapies have shown in patients with relapsed/refractory B-cell Acute Lymphoblastic Leukemia or Non-Hodgkin Lymphoma. These patients, for whom standard therapies have failed, have historically had dismal outcomes with survival measured in weeks or months. Remarkably, CAR-T therapy targeting CD19 has led to meaningful and durable remissions for large proportion of these patients in many different studies[1–7].

Currently, most genetically engineered Immune Effector Cell (IEC) therapies require several steps including i) manufacturing plasmid encoding the synthetic transgene and ancillary plasmids, ii) delivery of these plasmids into producer cells to generate virus, iii) collection of patient autologous T cells and integration of the transgene into the genomes of these cells by viral transduction, iv) expansion of the transduced T cells *ex vivo* to produce the therapeutic cells, v) extensive release-testing of the manufactured product, vi) preconditioning lymphodepletion of the patient, vii) infusion of the modified autologous cells, and viii) intensive clinical and immunological monitoring. Thus, there is considerable infrastructure and expertise required to deliver IEC treatments safely and successfully. The complexity of manufacturing IECs is a critical limitation to the cell therapy field, and a major contributor to the high cost of new cell-based interventions coming to market. Hence, there is considerable interest in the potential for "universal" alternative to autologous CAR-T products, with some encouraging results seen from gene-edited allo-CAR-Ts pre-clinically [8] and in case studies[9,10]. Likewise, the immortalized IEC cell line NK-92 has shown encouraging safety and efficacy in a recent phase 1 trial, but the requirement of irradiating the cells pre-infusion to reduce oncogenic risk will likely remain limiting for this approach.[11] The generation of a bank of allogeneic CAR-T cells by *in vitro* differentiation and maturation of hematopoietic stem and progenitor cell precursors is an alternative and highly compelling strategy. Demonstrated in principle, this approach awaits further optimization.[12]

In principle, universal IEC therapy could also be achieved by direct infusion of a gene transfer vector, such that cell manufacturing is sidestepped completely. Different approaches to *in vivo* gene delivery have been

explored, preclinically, for CAR-T therapy. Nanoparticles that carry a CAR transposon and that are coated with anti-CD3 targeting antibodies can transduce T cells *in vivo* yielding functional CAR-T cells[13], as can lipid nanoparticles that carry CAR mRNA and display anti-CD5 targeting antibodies[14]. Similarly, *in vivo* delivery of high doses of 10^{10} to 10^{11} lentiviral particles that bear CAR transgenes, and that have been pseudotyped to target either CD3+, CD8+ or CD4+ T cells, can yield functional CAR-T[15–17]. Here, we show efficient *in vivo* generation of functional CAR-T cells in wild-type mice upon infusion of lower doses (on the order of 10^6 to 10^7 particles) of conventional VSV-G lentivirus bearing transgenes that encode conventional FMC63 or ID3 anti-CD19 binding domains.

Results

During our early pre-clinical development of an anti-CD19 CAR intervention for B cell malignancies we explored how CAR-T cells behave *in vitro* in the context of antigen driven expansion. Using a standard 2nd generation anti-CD19 CAR design[18] (EF1α promoter, FMC63 scFv CD19 binding domain, CD8α hinge and transmembrane domain, 4-1BB co-stimulatory domain, CD3z signaling domain and 2A-GFP tag), we observed, as have many other investigators, that B cells drive robust expansion of functional CD19 CAR-T cells *in vitro*. This led us to explore *in vivo* transduction and expansion of CAR-T cells *in vivo* using a murine model system. We constructed a CAR where we changed the scFv binding domain from FMC63[19] (a monoclonal antibody raised against human CD19) to 1D3[20] (a monoclonal antibody raised against mouse CD19). To verify activity *in vitro*, 2.5×10^5 splenocytes from wildtype C57BL/6 mice were transduced with lentivirus encoding either the 1D3-CD19CAR-GFP (murine), FMC63-CD19CAR-GFP (human) or GFP-only transgene, then stimulated with a further excess of irradiated autologous murine splenocytes as a source of murine CD19 antigen. We observed that murine T-cells modified with either of the CARs expanded rapidly and selectively. Specifically, for murine T cells modified with the human CAR, expansion was 8.8+/- 0.03 (mean +/- SD) fold at day 63 relative to GFP transduced T cells ($p < 0.004$ paired, two-tail T test), and for murine T cells modified with the murine CAR

expansion was 12.9 +/- 0.09 fold at day 63, relative to GFP transduced T cells ($p < 0.002$ paired, two-tail T test). The murine control T cells transduced with GFP-only lentivirus showed very limited yet detectable expansion, possibly driven by the original CD3/CD28 activation prior to transduction [**Figures 1A and 1B**]**.** All expanded murine CAR-T cells showed robust and selective killing of murine B cells *in vitro*. Target murine B cells co-cultured with either effector 1D3-CD19CAR-GFP or FMC63-CD19CAR-GFP modified murine T cells showed 24.8 +/- 1.69% (mean +/- SD) and 18.5 +/- 1.08% of murine B cells were unviable (FVS780 positive) after the 5 hour co-culture, respectively [**Figure 1C**].

For further validation we used 1D3 and FMC63 CD19-blocking antibodies to assess murine CAR-T cell specificity for the mouse CD19 antigen expressed by the A20 cell line [**Figure 1D**], As a baseline, 38.8 +/- 0.71% (mean +/- SD) of the target A20 cells were unviable after a 4 hour co-culture with the effector 1D3-CD19CAR-GFP modified murine T cells with no blocking antibody present. Upon titration of 1D3 blocking antibody, the ability of the 1D3-CD19CAR-GFP modified murine T cells to target the A20 cells produced a decrease in unviable A20 cells to 19.7 +/- 0.28% (mean +/- SD), which was the level of background killing observed for murine T cells transduced with the GFP-only transgene, likely due to alloreactivity. Likewise, 41.1 +/- 0.92% (mean +/- SD) of the target A20 cells were unviable after a 4 hour co-culture of the effector FMC63-CD19CAR-GFP modified murine T cells with no blocking antibody present and 20.8 +/- 0.57% of the A20 cells upon titration of FMC63 antibody. Interestingly, these results confirm that the FMC63 scFv is able to bind murine CD19 to the degree necessary for functional CAR-T activation in this experimental system. To our knowledge this has not previously been reported.

We then administered lentivirus encoding each CAR or GFP-only lentivirus to C57BL/6 wild type mice (age 6-8 weeks) by tail vein infusion, and drew peripheral blood at regular intervals. For the following experiments, the number of mice per treatment group was 8 (n=8). In **Figure 2** and **Figure 4**, error bars

represent the standard deviation away from the calculated mean of each treatment group. We observed that GFP-expressing T cells appear in the blood of mice 3 weeks after the initial injection of 3.6-4x10^6 infectious units (IU) of either the 1D3- or FMC63-CD19CAR-GFP lentivirus, but not after injection of the same dose of GFP-only lentivirus **[Figure 2]**. Specifically, we saw emergence of a persistent 1D3-CD19CAR-GFP transduced $CD3^+$ T cell population beginning at week 3 that reaching a maximum of 13.5 +/- 0.58% (mean +/- SD) of the peripheral blood $CD3^+$ T cell population by week 5 [**Figure 2A-2C**]. This coincided with the loss of B cells, seen 5 weeks after the initial injection **[Figure 2C].** In experiments where we infused murine T cells modified with the FMC63-CD19CAR-GFP construct we also saw the emergence of a persistent FMC63-CD19CAR-GFP transduced $CD3^+$ T cell population beginning at week 5 that reached a maximum of 7.8 +/- 0.76% of the peripheral blood $CD3^+$ T cell population by week 5 **[Figure 2A-2C].** Again, this coincided with a loss of B cells, seen 5 weeks after the initial injection. This further confirms functional recognition of murine CD19 by FMC63 **[Figure 2C].** With either CAR, B cell aplasia was sustained until the end of the protocol (week 8). Mice treated with 3.6-4x10^6 IU of the GFP control lentivirus had no GFP expressing T cells and did not show the same B cell loss **[Figures 2A-2C].** We looked for GFP expression in immune cell subsets other than T cells, including the CD20/CD45R/B220 B cell population, $CD11b^+$ macrophage, and $CD335^+$ natural killer (NK) cells, but found that only T cells expressed the reporter GFP gene, indicative of CAR expression **[Figure 2D,2E].** Our interpretation of these results is that interaction between the *in vivo* transduced CAR-T cells and endogenous B cells drives CAR-T cell expansion and CAR-T mediated B cell depletion, resulting eventually in B cell aplasia. The only overt change to mice treated with either 1D3- or FMC63-CD19CAR lentivirus was a modest decrease in weight of 5.5 +/- 2.97% (mean +/- SD) and 3.6 +/- 1.78%, respectively over the first week after treatment [**Figure S6**].

To further assess *in vivo* transduced CAR-T cells from peripheral blood we used a panel of markers that included CD3, CD4, CD8, CD44, CD62L and CD127 [**Figure 4**]. A gating strategy for the use of these markers

to define T cell immunophenotypes has been previously described [21,22], and an example of our implementation is illustrated in **Figure S5** and **Table S5.** At both timepoints tested (week 5 and week 8), we saw that $CD8^+$ CAR-T cells were more prevalent than $CD4^+$ CAR-T cells, and displayed mainly effector ($CD44^{high}$, $CD62L^{low}$ $CD127^{low}$) or effector memory ($CD44^{high}$, $CD62L^{low}$ $CD127^{high}$) phenotypes. Interestingly, these ID3 CAR-T cells proliferated sooner, and to a greater abundance than the FMC63 CAR-T cells, which did not become prominent until week 8. A small (<1%) but measurable population of GFP expressing $CD4^+$ $FOXP3^+$ regulator T cells was also observed at both timepoints. We conducted qPCR (Taqman) analysis to test for the presence of the CD19CAR transgene in additional tissues obtained 2 or 6 weeks after infusing mice with either of two different doses (2×10^7 or 2×10^6 IU) of the 1D3-CD19CAR-GFP virus. For the following experiments, the number of mice per treatment group was 7 (n=7). In **Figure 3**, error bars represent the standard deviation away from the calculated mean of each treatment group. From PBMC and spleen samples from treated mice we isolated DNA from three sorted cell populations: a T cell (CD3+) population, a B cell (CD20+) population, and an NK/NK-T and Macrophage (CD335+/CD11b+) population. We also isolated DNA from lung, ovary, bone marrow, and liver from these mice. At 6 weeks, mice treated with 2×10^6 IU of virus showed a relative quantity of 132.7 +/- 27.8 in PBMC-derived $CD3^+$ T cells and 131.0 +/- 35.4 in Spleen-derived $CD3^+$ T cells, while mice treated with 2×10^7 IU virus showed a relative quantity of 129.9 +/- 34.8 in PBMC-derived $CD3^+$ T cells and 147.1 +/- 41.4 in Spleen isolated $CD3^+$ T cells. Interestingly, at the earlier 2 week timepoint, qPCR analysis identified transduced T cells from PBMC and spleen in two of the six mice that were treated with the higher dose of 2×10^7 IU of virus , suggesting that higher T cell transduction can promote the earlier appearance of a sizeable transduced T cell population, although only sporadically. None of the off target cell types or tissues were qPCR positive for the transgene at any of the doses or timepoints [**Figure 3**].

Discussion

There have been no previously published reports of FMC63 crossreactivity, or that FMC63 is human specific. Zola et al.[19] initially characterized the FMC63 antibody as a mouse-human chimera with FMC63 mouse sequences for the VDJ (heavy) and VJ (light) chains with a human C region gene of IgG1, which was then tested for its ability to bind human CD19 compared to normal FMC63. Pietersz et al.[23] compared the mouse/human chimera FMC63 scFv for its ability to reduce human B cell tumours by 30% in scid/scid mice and found it similar to the mouse FMC63. Initial construction of the single chain Fv (scFv) of FMC63 [19] tested the scFv only against human cell lines. Construction of an anti-CD19 chimeric antigen receptor using this scFv [24]tested specifically against human PBMCs. Evolution of the anti-CD19 chimeric antigen receptor designs [25,26] tested against human CD19 tumours (NALM cell lines) but not against mouse cell lines. Evaluation of the chimeric antigen receptor-modified T cells [27]tested only against human cell lines and patient samples. None of these tested the effect of FMC63 against mouse CD19. The region of the FMC63 epitope (aa 155-172 [28]) has 75% amino acid identity and 83% amino acid similarity in human and mouse and structural prediction shows conserved conformation of this region (Figure S7).

Interestingly, murine T cells have previously been demonstrated to have lower transduction efficiencies, compared to human T cells and compared to other murine cell types [29–32], when transduced with HIV-1 based lentiviral vectors. The viral vector system we describe here avoids some of the known barriers of murine T cells. The entry block is avoided by the use of VSV-G pseudotyped virus. Reduced Tat activation is avoided entirely by our use of a Tat-independent transfer vector with a chimeric Rous Sarcoma virus LTR. Reduced LTR promoter activity is compensated by the use of an internal EF1α promoter driving the transgene. Some reduction in lentiviral integration may still be expected in murine T cells due to inefficient nuclear import of the pre-integration complex.[31] Empirically, however, we find that while our lentiviral vectors transduce murine T

cells less efficiently than they transduce human T cells **[Figures S2]**, the level of transduction of murine T cells *in vitro* and *in vivo* is sufficient.

Quantitative PCR analysis at weeks 2 and 6 post initial injection, of T cells (CD3), B cells (CD20), NK/NK-T cells (CD335 and CD11b) as well as liver, lung, ovaries, and bone marrow tissue, showed that only the T cells had detectable CAR transgene. We did not look at the *in vivo* transduction of progenitor / stem cell types like $CD34^+$ hematopoietic stem and progenitor cells or endothelial / vascular cell types. We expect that transduction events at our administered doses are below the limit of our detection, and that the transduction of the T cells are only detectable due to antigen driven CAR-T cell expansion. Indeed, only in the higher delivered viral dose, do we see any CAR transgene in the PBMC and spleen CD3+ T cells at the two week timepoint (**Figure 3**). Previous studies have reported transduction of hepatocytes by VSV-G pseudotyped lentiviral particles [33,34] when used in other settings. The substantially lower viral doses ($2.04x10^7$ IU and $2.04x10^6$ IU per mouse) used in our study does not yield detectable levels of CAR transgene in other tissues. We would expect that B cells, NK/NK-T cells and macrophages, express low levels of LDL-R and thus the transduction of these cells by VSV-G lentivirus *in vivo* would be expected to be low [35] in accord with our lack of CAR transgene detection in these cells. However, given that other LDL-R bystander cell populations will act as viral sinks, and given that VSV-G lentiviruses are inactivated by human complement [36], optimal dosing regimens will need to be defined empirically.

Further implications to the transduction of bystander cells are unique to the setting of anti-CD19 CAR-T therapy. For example, expression of the CAR transgene in malignant B cells by inadvertent transduction of tumor blasts is potentially problematic, because the CAR can bind CD19 antigen on the same cell and block engagement by cytolytic CAR-T cells. This is a known but rare mechanism of relapse in conventional *ex vivo* protocols [37]. Another consideration is that while receptor transgene expression in $CD8^+$ cytolytic T cells and $CD4^+$ helper T cells is desirable,[38] expression in regulatory T cells may have a non-negligible inhibitory

effect on CAR-T cell immunoreactivity over time. Utilizing modified promoters that drive CAR transgene expression in effector but not regulatory T cells is one strategy for overcoming this potential problem.

Insertional mutagenesis of integrating viral vectors led to highly regrettable negative outcomes in early gene therapy trials and severe setbacks to the gene therapy field. [39–44] All of these clinical trials involved *ex-vivo* gene transfer to hematopoietic stem cells using "first generation" gamma-retroviral vectors. Retrospective analysis has shown that the mechanism of leukemogenesis was oncogene overexpression driven by integration, in the vicinity of oncogenes, of viral vectors bearing strong promoters in their long terminal repeats. The advent of self-inactivating lentiviral vectors with transgene expression driven by mammalian (not viral) LTR promoters (as used in the present study) have mitigated oncogenic risk [45,46] and are now routinely used in different disease settings without incident, and no detrimental effects of insertional mutagenesis have been reported from any CAR-T clinical trial using retroviral vectors to date. Still, before clinical testing of *in vivo* CAR-T transduction could be considered, the risk of insertional mutagenesis must be fully mitigated.

The use of HIV-based lentivirus for gene transfer also raises concern about the theoretical risk of transmission of replication competent lentivirus (RCL). We use a modified 2nd generation lentiviral vector system with the minimal viral components included in the 3rd generation system split across three plasmids instead of four. These alterations abolish the potential for recombination events that can lead to formation of RCL in target cells. Testing of hundreds of cell therapy products generated with third generation vectors as well screening clinical trial participants after infusion of cell product failed to detect RCL, [47,48] demonstrating the safety of lentiviral gene therapy in this regard.

Clinical CAR-T protocols and other clinical IEC protocols typically include lymphodepleting chemotherapy with cyclophosphamide and/or fludarabine as pre-conditioning. While it would not be productive to perform complete lymphoablation prior to a viral infusion protocol (because endogenous T cells must be present for virus to transduce), mild preconditioning may be beneficial, if depletion leaves enough endogenous

T cells in circulation to support viral transduction and conversion to CAR-Ts, while at the same time providing a niche for robust CAR-T expansion and engraftment [49]. This could be further tested, but may be unnecessary given our results show full ablation of endogenous B cells after lentiviral infusion **[Figure 2C]** without any pre-conditioning lymphodepletion.

In summary, anti-CD19 CAR-T therapy for B cell malignancies has shown clinical success, but a major limitation is the logistical complexity and high cost of manufacturing autologous cell products. This has led to increasing interest in industry and academia in universal (non-personalized) strategies. Here we report that intravenous infusion of replication-incompetent VSVG-pseudotyped lentiviral particles carrying an anti-CD19 CAR transgene with either an FMC63 or ID3 anti-CD19 binding domain can effectively transduce murine T cells, leading to CAR-T proliferation and subsequent CAR-T mediated B cell aplasia. Out study supports the notion that CAR-T cells expanded *in vivo* could be effective against B cell malignancies, which requires further study. This observation also supports this modality as a potential universal CAR-T intervention, that could have clinical relevance if further engineering is able to overcome the safety concerns and other limitations of systemic viral gene therapy.

Materials and Methods

Media

RPMI-1640 supplemented media (sRPMI-1640) consisted of 2 mM GlutaMAX (Invitrogen, 35050-061), 1 mM MEM non-essential amino acid (Invitrogen, 11140-050), 1 mM sodium pyruvate (Invitrogen, 11360-070), 10 mM HEPES (Invitrogen, 15630-808), 100 U/mL penicillin- streptomycin (Invitrogen, 15140-122), MycoZap prophylactic (Lonza, VZA-2031), 0.05mM 2-Beta Mercaptoethanol (Sigma, 60-42-2, 2-βME added to media for murine cell cultures only) and 10% heat-inactivated fetal bovine serum (Invitrogen, 12484-028). For expansion cultures IL-2 (StemCell, 78036.3 or Miltenyi Biotech, 130-097-745) was added to the

sRPMI-1640 media. Cells were cultured in sRPMI-1640 with a final IL-2 concentration of 300IU/ml, unless otherwise stated. FACS media consisted of 1x D-PBS (Sigma, 59331C) with 2% HI-FCS. In house MACS separation buffer consisted of D-PBS with 2mM EDTA (ThermoFisher, 15575020) and 2% HI-FBS.

Production of lentiviral gene transfer vectors.

Our lentivector system is a modified 2nd generation system that uses three separate plasmids to split the lentiviral genome as previously described.[50,51] The system is comprised of a packaging plasmid encoding gag, pol and rev, a VSV-G envelope expressing plasmid and a transfer plasmid encoding the transgene. Biosafety of the 2nd generation design was improved by removal of tat from the packaging plasmid with the concurrent replacement of the transfer vector 5' Long terminal repeat (LTR) with chimeric sequence for Tat-independent expression and a self-inactivating modified 3' LTR.[52] These modifications serve to prevent the formation of replication competent virus. Synthetic transgene sequences encoding 1) GFP, 2) FMC63-CD19CAR-2A-GFP and 3) 1D3-CD19CAR-2A-GFP were manufactured (ATUM) containing the FMC63 (anti-human) or 1D3 (anti-mouse) anti-CD19 scFv with human co-stimulatory 4-1BB activation domains as a chimeric antigen receptor, subcloned into the transfer plasmid and verified by Sanger sequencing (Genewiz). Envelope (VSV-G) and packaging (GagPolRev) plasmids were also manufactured (ATUM). To manufacture virus particles, envelope, packaging, and transfer plasmids were co-transfected into the packaging cell line HEK-293T (clone 17; ATCC) using TransIT-LT1 (Mirus, MIR2305). Media containing the lentivirus was collected after transfection, filtered and then ultracentrifuged at 25,000 rpm or 106,750 xg, for 90 minutes at 4˚C (Optima XE-90, Beckman-Coulter with SW 32 Ti swinging bucket rotor) to pellet the virus. Viral pellets were resuspended in 1x D-PBS and aliquoted for long term storage at -80C. Functional viral titers were established by infection of K562 cells (ATCC) and EL4 cells (ATCC) determined by transducing $5x10^4$ EL4 or K562 cells (ATCC) with 1, 2, 4, 8, 16, or 32 µL of concentrated viral supernatant. Performed in duplicate, cells

were suspended in a final volume of 500µL of sRPMI-1640 media, in the 24-well format. Cells were then incubated for 72 hours, before being washed, centrifuged, and resuspended in FACS media. Acquisition was performed on the BD LSRFortessa cell analyser, and analysed using FlowJo and GraphPad Prism software version 8.0.0 for windows (GraphPad Software, California, USA) [**Figure S1]**.

Sample acquisition and storage.

Human PBMCs were isolated by Ficoll gradient purification as per manufactures protocol (Ficoll, GE-17-1440, GE Healthcare) from human peripheral blood leukapheresis pack (StemCell). 100-150µl of C57BL/6 mouse blood was collected in lithium heparin capillary tubes via tail vein blood sampling pre-treatment and then every week post-treatment for 8 weeks. The blood samples were diluted with 1 - 1.5 ml of cold RPMI, which was overlayed with 4ml of Ficoll and C57BL/6 mouse PBMCs were isolated following the manufacturer's protocol. C57BL/6 mouse PBMCs were isolated and analysed within 24 hours of isolation. PBMCs were resuspended in sRPMI-1640 at a concentration of $1x10^6$ cells per ml, placed into a T25 culture flask (156367, ThermoFisher), and rested overnight in the cell incubator at 37˚C with 5% CO_2 airflow before being used in any analysis. Human PBMCs and C57BL/6 mouse PBMCs not immediately used in any experiments were stored down by resuspending cells in freezing media (HI-FBS with 10% DMSO, Fisher Scientific, BP231-100) in aliquots of 5-10 $x10^6$ cells per ml and frozen down to -80˚C at a speed of 1˚C/min prior to storage in liquid nitrogen.

The C57BL/6 mouse splenocytes used in the *in vitro* assays were acquired from naive or untreated C57BL/6 mice, aged 4-8 weeks old. All C57BL/6 mice were however processed the same way by first manually dissociating the spleens and filtering them through a 70 µm cell strainer (Corning, CLS431751) into a 50mL falcon tube, centrifuging 400xg for 10 min (Eppendorf Centrifuge 5810R, rotor A-4-62) at room temperature to pellet the cells. The splenocytes samples were resuspended in 5mL of ACK (Ammonium-Chloride-Potassium)

Lysing Buffer (ThermoFisher), before incubating the cells on ice for no longer than 4 minutes. 10 mL of sRPMI-1640 media was added to the cells to neutralize the ACK buffer and wash the splenocytes. The splenocytes were then centrifuged at 400xg for 10 min (Eppendorf Centrifuge 5810R, rotor A-4-62) at room temperature, the supernatant was removed, and the splenocytes washed again before being resuspended in sRPMI-1640 media and cell numbers obtained using the Countess automated cell counter (ThermoFisher). Splenocytes were stored down by resuspending cells in freezing media (HI-FBS with 10% DMSO, Fisher Scientific, BP231-100) in aliquots of 5-10 x10^6 cells per ml and frozen down to -80˚C at a speed of 1˚C/min prior to storage in liquid nitrogen.

The acquired bone marrow, ovaries, lung, and liver tissues were manually dissociated and filtered through a 70 μm cell strainer (Corning, CLS431751) into a 50mL falcon tube. Samples were then, washed with PBS and centrifuged at 400xg for 10 min (Eppendorf Centrifuge 5810R, rotor A-4-62) at room temperature to pellet the cells. The cells were counted and stored in RNA later (AM7021, ThermoFisher) following the manufactures protocols. DNA was extracted from these samples using the DNeasy Blood and Tissue kit (Qiagen, 69504) and following the manufacturer's protocol.

In vitro 1D3- and FMC63-CD19CAR-GFP modified T cell expansion and testing using C57BL/6 mouse splenocytes

C57BL/6 mouse splenocytes were removed from liquid nitrogen storage, thawed, and resuspended in sRPMI-1640 with 300 IU/ml of IL-2, and 30ng/ml of CD3 (clone 145-2C11, 100314, BioLegend) and 30ng/ml CD28 (clone 37.51, 102112, BioLegend) antibodies, at a concentration of 1x10^6 cells/ml. The splenocytes were then treated with 1D3-, FMC63-CD19CAR-GFP, or GFP-only viral supernatant at a MOI of 5 (calculated based on titration data) and incubated for 72 hours. Following transduction, cells were washed by resuspending the cells in sRPMI-1640, centrifuging them at 400xg for 10 mins at room temperature (Eppendorf Centrifuge 5810R, rotor A-4-62), removing the supernatant, and repeating the process a further 2 times. The cells were

resuspended in sRPMI-1640 media containing 300IU/ml of IL-2 at a concentration of $2.5x10^5$ cells per ml, with 1 ml being aliquoted per well, in the 6-well culture plate format. Irradiated autologous murine splenocytes (50Gy) were resuspended in sRPMI-1640 media containing 300IU/ml of IL-2 at a concentration of $2.5x10^7$/ml and 1 ml was added to the transduced splenocytes giving a final ratio of 1:100 transduced splenocytes to irradiated splenocytes. Every third day, 1ml of the culture media was removed and 1ml of fresh sRPMI-1640 media with 600IU/ml of IL-2 was added (giving a final concentration of 300IU/ml IL-2). On days 0, 14, 28, and 63, the cells were counted using the Countess automated cell counter (ThermoFisher) and an aliquot of $3x10^4$ cells were stained with fluorescent labeled antibodies and analyzed using flow cytometry [**Figure 1A** and **1B**].

In a 96-well plate format with a final volume of 200µl (sRPMI-1640), $1x10^5$ 1D3-, FMC63-CD19CAR, or GFP-transduced T cells from day 63 of the expansion were co-cultured for 5 hours with $1x10^5$ B cells isolated from another sample of C57BL/6 mouse splenocytes, using the Miltenyi MACS mouse CD19 B-cell isolation beads, following the manufacturer's protocol and using a MACS separation buffer made in-house. At the end of the co-culture, the cells were stained with fluorescent labeled antibodies and analyzed using flow cytometry [**Figure 1C**]. Cells were washed with 500µl of D-PBS and centrifuged at 400xg for 10 minutes at room temperature (Eppendorf Centrifuge 5810R, rotor A-4-62). The supernatant was removed and the cell pellet resuspended in 50µl of D-PBS before being stained with CD20-PE (clone A1SB12, 12-0201-82, eBioscience), CD3-efluor 450 (clone 17A2, 48-0032-82, eBioscience), and the non-viable cell marker, Fixable Viability Stain 780 (FVS780) (565388, BD Biosciences). Cells and antibodies were incubated at 4ºC for 30 min, then washed by adding 2mL of FACS media to each tube and centrifuging for 10 minutes at 400xg at 4˚C followed by removal of the supernatant before resuspension in 500µl of cold FACS media. Flow cytometry acquisition was performed using the BD LSRFortessa cell analyser with BD FACSDiva software. The analysis was performed using FlowJo software, version 10 for windows and GraphPad Prism software version 8.0.0 for windows (GraphPad Software, California, USA) [**Figure S3** and **Table S1**].

In vitro 1D3- and FMC63-CD19CAR-GFP modified mouse T cells co-culture with A20 cells.

C57BL/6 mouse splenocytes were transduced with 1D3-, FMC63-CD19CAR-GFP, or GFP-only viral supernatant, sorted, and expanded as previously mentioned. The murine, CD19 expressing, A20 cell line (ATCC) was used as the target cells in a co-culture with the sorted and expanded 1D3-, FMC63-CD19CAR-GFP, or GFP-only expressing murine T cells. In order to verify the ability for both the 1D3- and FMC63-CD19CAR to target the mouse CD19 antigen, the A20 cells were incubated with 10, 1, 0.1, 0.001, 0 µg/ml of either the 1D3-CD19 blocking antibody (152402, BioLegend) or the FMC63-CD19 blocking antibody (NBP2-52716, Novus Biologicals). In the 96-well plate format with a final volume of 200µl (sRPMI-1640) the A20 cells were then co-cultured the 1D3-, FMC63-CD19CAR-GFP, or GFP-only expressing murine T cells at an effector to target of 4:1($2x10^5$:$5x10^4$), for 4 hours. Cells were then washed and stained with CD20-PE, CD3-efluor 450, and the non-viable cell marker, Fixable Viability Stain 780 (FVS780) as previously described [**Figure S3** and **Table S2**]. Flow cytometry acquisition was performed using the BD LSRFortessa cell analyser with BD FACSDiva software. The analysis was performed using FlowJo software, version 10 for windows and GraphPad Prism software version 8.0.0 for windows (GraphPad Software, California, USA) [**Figure 1D**].

In vivo testing.

All animal experiments were assessed and approved by the University of British Columbia's Animal Care Committee under ethics certificate #A17-0107. For the *in vivo* testing, C57BL/6 mice, aged 4 to 8 weeks old, were obtained from the BC Cancer Research Centre's Animal Resource Centre. The experimental mice received one tail vein infusion on day 1 which involved the intravenous injection of 200µl of D-PBS containing 3.6-$4x10^6$ total infectious units of either 1D3-, FMC63-CD19CAR-GFP, or GFP-only. For subsequent dose response *in vivo* experiments, mice received an intravenous injection of 200µl of D-PBS containing either $2.04x10^6$ or $2.04x10^7$ total infectious units of 1D3-CD19CAR-GFP. Mice were monitored closely for the first 72

hours, and then once a day until the experimental endpoint. The mice were also weighed periodically and blood collected in lithium heparin capillary tubes via tail vein sampling as previously described. At the experimental endpoint, the mice were humanly euthanized and spleen and blood tissue collected and processed as previously described. The cells were stained with fluorescent labeled antibodies and analyzed using flow cytometry [**Figure 2** and **Figure 4**]. DNA from the cells of the various tissues was collected and the samples analyzed for CD19CAR-GFP possession using qPCR [**Figure 3**].

For flow cytometry acquisition and analysis, $4x10^5$ cells were stained with CD3-efluor 450 (clone 17A2, 48-0032-82, eBioscience), CD90.2-AF700 (clone 30-H12, 105319, BioLegend), CD20-PE (clone A1SB12, 12-0201-82, eBioscience), CD45R/B220-APC-CY7 (clone RA3-6B2, 103223, BioLegend), CD335-APC (clone 29A1.4, 137608, BioLegend), and CD11B-BV605 (clone M1/79, 101237, BioLegend) conjugated flow antibodies. Cells and antibodies were incubated at 4ºC for 30 min, then washed by adding 2mL of FACS media to each tube and centrifuging for 10 minutes at 400xg at 4˚C, discarding the supernatant before resuspension in 500µl of cold FACS media. Acquisition was performed on the BD LSRFortessa cell analyser, and analysed using FlowJo and GraphPad Prism software version 8.0.0 for windows (GraphPad Software, California, USA) [**Figure S4**, **Table S3** and **Table S4**].

In the immunophenotyping analysis [**Figure 4**], up to $5x10^4$ cells were stained with CD3-efluor 450 (clone 17A2, 48-0032-82, eBioscience), CD4-PE (clone GK1.5, 100408, BioLegend), CD8-BUV395 (clone QA17A07, 155006, BioLegend), CD44-alexa fluor 700 (clone IM7, 103026, BioLegend), CD62L-PerCP-CY5.5 (clone MEL-14, 104432, BioLegend), CD127-APC-CY7 (clone A7R34, 135040, BioLegend), CD25-PE-CF594 (clone PC61, 562694, BD Biosciences), and FOXP3-APC (clone FJK-16s, 563786, BD Biosciences) and incubated at 4ºC for 30 min, as previously mentioned. The cells were then fixed, by incubating the cells in up to 200µL of fixation buffer (420801, BioLegend) at 4ºC for 30 min. The cells were than washed by adding 2mL of FACS media and centrifuging for 10 minutes at 400xg at 4˚C, and resuspended in 1x Intracellular

Staining Perm Wash Buffer (10x stock solution, diluted to 1x with ddH_2O, 420801, BioLegend) at 4ºC for 30 min, before being stained with FOXP3-APC (at 4ºC for 30 min). Again cells were washed by adding 2mL of FACS media and centrifuging for 10 minutes at 400xg at 4˚C, discarding the supernatant before resuspension in 500µl of cold FACS media. Acquisition was performed on the BD LSRFortessa cell analyser, and analysed using FlowJo and GraphPad Prism software version 8.0.0 for windows (GraphPad Software, California, USA) [**Figure S5 and Table S5**]. For all flow analyses, we used the CD20-PE antibody as a B cell marker in place of a CD19 antibody [**Figure 1** and **Figure 2**] to avoid any possible interference between anti-CD19 antibody and anti-CD19 CARs in these mixed cell populations.

Quantitative PCR of DNA isolated from mouse tissues.

Spleens and PBMC from 2 and 6 weeks post 1D3-CD19CAR-LV treatment were sorted into CD3, CD20, and CD335/CD11b expressing cell types using BD FACSAria and BD FACSDiva software [**Figure S4**]. DNA was then extracted from the spleen and PBMC sorted cell subtypes, along with the DNA from liver, ovaries, lung, and bone marrow tissues (stored in RNA later) was collected using the DNeasy Blood and Tissue kit (Qiagen, 69504) following the manufacturer's protocol. The DNA concentrations were read using NanoDrop 8000 Spectrophotometer (ND-8000-GL, ThermoFisher) by following the manufacturer’s protocol. The DNA concentration was normalized to a concentration of 19-21ng/µl. To detect the presence of the CD19CAR gene, using a Taqman primer probe set which amplifies DNA from the co-stimulatory and activation domains of the 1D3-CD19CAR-T transgene. For every 2µl of template DNA, 0.5µl of the CD19CAR [44] and murine-β actin Taqman assay sets (4352341, ThermoFisher), 5µl of Taqman Fast Advanced 364 Master Mix (4444557, Invitrogen), brought to a final volume of 10µl, with ultrapure water (10977023, Invitrogen). Thermocycling was done using the QuantStudio 6 Flex System, in the 384-Well format, using the comparative Ct (ΔΔCt) set up.

Thermocycling conditions: one cycle at 50°C for 2 min; 1 cycle at 95°C for 2 min, 368 then 95°C for 2 sec and 60°C for 20 sec for 40 cycles, capturing data at the end of every cycle. For the analysis, the mouse β-Actin gene was used as the endogenous control and an *in vitro* transduced spleen sample, positive for 1D3-CD19CAR-GFP possession, was used as a positive control. Spleen cells from an untreated mouse was used as the reference control for the ΔΔCT calculation required to obtain a relative quantity.

Thermocycling was done using the QuantStudio 6 Flex System, in the 384-Well format, using the comparative Ct (ΔΔCt) set up. Thermocycling conditions: one cycle at 50°C for 2 min; 1 cycle at 95°C for 2 min, then 95°C for 3 sec and 60°C for 30 sec for 40 cycles, capturing data at the end of every cycle. For the analysis, the mouse β-Actin gene was used as the endogenous control and the $CD3^+$ PBMC and Spleen from PBS treated mouse from week 1 and week 8 were used as the reference control, as these samples showed the lowest relative quantity, as they were treated with PBS.

Author Contributions and Notes

R.A.H, C.M.R and E.Y. designed research, C.M.R, E.Y, L.D., and D.J.W. performed research, C.M.R and S.D.B. analyzed data; all authors prepared and edited the manuscript.

The authors declare no conflict of interest.

Acknowledgments

This research was supported by the British Columbia Cancer Foundation, the Leon Judah Blackmore Foundation and the BioCanRx network.

Keywords

CAR-T, Immune effector cells; viral vector, gene transfer, gene therapy, leukemia, lymphoma

01

02

References

1. Neelapu SS, Locke FL, Bartlett NL, Lekakis LJ, Miklos DB, Jacobson CA, Braunschweig I, Oluwole OO, Siddiqi T, Lin Y, Timmerman JM, Stiff PJ, Friedberg JW, Flinn IW, Goy A, Hill BT, Smith MR, Deol A, Farooq U, McSweeney P, Munoz J, Avivi I, Castro JE, Westin JR, Chavez JC, Ghobadi A, Komanduri K V., Levy R, Jacobsen ED, Witzig TE, Reagan P, Bot A, Rossi J, Navale L, Jiang Y, Aycock J, Elias M, Chang D, Wiezorek J, Go WY. Axicabtagene ciloleucel CAR T-cell therapy in refractory large B-Cell lymphoma. N Engl J Med. 2017 Dec 28;377(26):2531–44.
2. Maude SL, Laetsch TW, Buechner J, Rives S, Boyer M, Bittencourt H, Bader P, Verneris MR, Stefanski HE, Myers GD, Qayed M, De Moerloose B, Hiramatsu H, Schlis K, Davis KL, Martin PL, Nemecek ER, Yanik GA, Peters C, Baruchel A, Boissel N, Mechinaud F, Balduzzi A, Krueger J, June CH, Levine BL, Wood P, Taran T, Leung M, Mueller KT, Zhang Y, Sen K, Lebwohl D, Pulsipher MA, Grupp SA. Tisagenlecleucel in children and young adults with B-cell lymphoblastic leukemia. N Engl J Med. 2018 Feb 1;378(5):439–48.
3. Park JH, Rivière I, Gonen M, Wang X, Sénéchal B, Curran KJ, Sauter C, Wang Y, Santomasso B, Mead E, Roshal M, Maslak P, Davila M, Brentjens RJ, Sadelain M. Long-term follow-up of CD19 CAR therapy in acute lymphoblastic leukemia. N Engl J Med. 2018 Feb 1;378(5):449–59.
4. Hay KA, Gauthier J, Hirayama A V., Voutsinas JM, Wu Q, Li D, Gooley TA, Cherian S, Chen X, Pender BS, Hawkins RM, Vakil A, Steinmetz RN, Schoch G, Chapuis AG, Till BG, Kiem HP, Ramos JD, Shadman M, Cassaday RD, Acharya UH, Riddell SR, Maloney DG, Turtle CJ. Factors associated with durable EFS in adult B-cell ALL patients achieving MRD-negative CR after CD19 CAR T-cell therapy. Blood. 2019 Apr 11;133(15):1652–63.
5. Hirayama A V, Gauthier J, Hay KA, Voutsinas JM, Wu Q, Pender BS, Hawkins RM, Vakil A, Steinmetz RN, Riddell SR, Maloney DG, Turtle CJ. High rate of durable complete remission in follicular lymphoma after CD19 CAR-T cell immunotherapy. Blood [Internet]. 2019 Aug 15 [cited 2020 Apr 21];134(7):636–40. Available from: http://www.ncbi.nlm.nih.gov/pubmed/31648294
6. Schuster SJ, Svoboda J, Chong EA, Nasta SD, Mato AR, Anak Ö, Brogdon JL, Pruteanu-Malinici I, Bhoj V, Landsburg D, Wasik M, Levine BL, Lacey SF, Melenhorst JJ, Porter DL, June CH. Chimeric antigen receptor T Cells in refractory B-Cell lymphomas. N Engl J Med. 2017 Dec 28;377(26):2545–54.
7. Grigor EJM, Fergusson D, Kekre N, Montroy J, Atkins H, Seftel MD, Daugaard M, Presseau J, Thavorn K, Hutton B, Holt RA, Lalu MM. Risks and Benefits of Chimeric Antigen Receptor T-Cell (CAR-T) Therapy in Cancer: A Systematic Review and Meta-Analysis. Vol. 33, Transfusion Medicine Reviews. W.B. Saunders; 2019. p. 98–110.
8. Sommer C, Boldajipour B, Kuo TC, Bentley T, Sutton J, Chen A, Geng T, Dong H, Galetto R, Valton J, Pertel T, Juillerat A, Gariboldi A, Pascua E, Brown C, Chin SM, Sai T, Ni Y, Duchateau P, Smith J, Rajpal A, Van Blarcom T, Chaparro-Riggers J, Sasu BJ. Preclinical Evaluation of Allogeneic CAR T Cells Targeting BCMA for the Treatment of Multiple Myeloma. Mol Ther [Internet]. 2019 Jun 5 [cited 2020 Apr 22];27(6):1126–38. Available from: http://www.ncbi.nlm.nih.gov/pubmed/31005597
9. Qasim W, Zhan H, Samarasinghe S, Adams S, Amrolia P, Stafford S, Butler K, Rivat C, Wright G, Somana K, Ghorashian S, Pinner D, Ahsan G, Gilmour K, Lucchini G, Inglott S, Mifsud W, Chiesa R, Peggs KS, Chan L, Farzeneh F, Thrasher AJ, Vora A, Pule M, Veys P. Molecular remission of infant B-ALL after infusion of universal TALEN gene-edited CAR T cells. Sci Transl Med [Internet]. 2017 Jan 25 [cited 2020 Apr 22];9(374). Available from: http://www.ncbi.nlm.nih.gov/pubmed/28123068
10. Brudno JN, Somerville RPT, Shi V, Rose JJ, Halverson DC, Fowler DH, Gea-Banacloche JC, Pavletic SZ, Hickstein DD, Lu TL, Feldman SA, Iwamoto AT, Kurlander R, Maric I, Goy A, Hansen BG, Wilder JS, Blacklock-Schuver B, Hakim FT, Rosenberg SA, Gress RE, Kochenderfer JN. Allogeneic T Cells That Express an Anti-CD19 Chimeric Antigen Receptor Induce Remissions of B-Cell Malignancies That Progress After Allogeneic Hematopoietic Stem-Cell Transplantation Without Causing Graft-Versus-Host Disease. J Clin Oncol [Internet]. 2016 Apr 1 [cited 2020 Apr 22];34(10):1112–21. Available from: http://www.ncbi.nlm.nih.gov/pubmed/26811520
11. Williams BA, Law AD, Routy B, DenHollander N, Gupta V, Wang X-H, Chaboureau A, Viswanathan S, Keating A. A phase I trial of NK-92 cells for refractory hematological malignancies relapsing after autologous hematopoietic cell transplantation shows safety and evidence of efficacy. Oncotarget [Internet]. 2017 Oct 24;8(51):89256–68. Available from: http://www.ncbi.nlm.nih.gov/pubmed/29179517
12. Shukla S, Langley MA, Singh J, Edgar JM, Mohtashami M, Zúñiga-Pflücker JC, Zandstra PW. Progenitor T-cell differentiation from hematopoietic stem cells using Delta-like-4 and VCAM-1. Nat Methods. 2017 Apr 27;14(5):531–8.
13. Smith TT, Stephan SB, Moffett HF, McKnight LE, Ji W, Reiman D, Bonagofski E, Wohlfahrt ME, Pillai SPS, Stephan MT. In situ programming of leukaemia-specific T cells using synthetic DNA nanocarriers. Nat Nanotechnol [Internet]. 2017;12(8):813–20. Available from: http://www.ncbi.nlm.nih.gov/pubmed/28416815
14. Aghajanian H, Kimura T, Rurik JG, Hancock AS, Leibowitz MS, Li L, Scholler J, Monslow J, Lo A, Han W, Wang T, Bedi K, Morley MP, Linares Saldana RA, Bolar NA, McDaid K, Assenmacher C-A, Smith CL, Wirth D, June CH, Margulies KB, Jain R, Puré E, Albelda SM, Epstein JA. Targeting cardiac fibrosis with engineered T cells. Nature [Internet]. 2019;573(7774):430–3. Available from: http://www.ncbi.nlm.nih.gov/pubmed/31511695
15. Pfeiffer A, Thalheimer FB, Hartmann S, Frank AM, Bender RR, Danisch S, Costa C, Wels WS, Modlich U, Stripecke R, Verhoeyen E, Buchholz CJ. In vivo generation of human CD 19□ CAR T cells results in B□cell depletion and signs of cytokine release syndrome . EMBO Mol Med. 2018 Nov;10(11).
16. Frank AM, Braun AH, Scheib L, Agarwal S, Schneider IC, Fusil F, Perian S, Sahin U, Thalheimer FB, Verhoeyen E, Buchholz CJ. Combining T-cell-specific activation and in vivo gene delivery through CD3-targeted lentiviral vectors. Blood Adv [Internet]. 2020;4(22):5702–15. Available from: http://www.ncbi.nlm.nih.gov/pubmed/33216892
17. Agarwal S, Hanauer JDS, Frank AM, Riechert V, Thalheimer FB, Buchholz CJ. In Vivo Generation of CAR T Cells Selectively in Human CD4+ Lymphocytes. Mol Ther [Internet]. 2020;28(8):1783–94. Available from: http://www.ncbi.nlm.nih.gov/pubmed/32485137
18. Imai C, Mihara K, Andreansky M, Nicholson IC, Pui C-HH, Geiger TL, Campana D. Chimeric receptors with 4-1BB signaling capacity provoke potent cytotoxicity against acute lymphoblastic leukemia. Leukemia [Internet]. 2004 Apr [cited 2020 May 4];18(4):676–84.

Available from: http://www.ncbi.nlm.nih.gov/pubmed/14961035
19. Nicholson IC, Lenton KA, Little DJ, Decorso T, Lee FT, Scott AM, Zola H, Hohmann AW. Construction and characterisation of a functional CD19 specific single chain Fv fragment for immunotherapy of B lineage leukaemia and lymphoma. Mol Immunol [Internet]. 1997 Nov 1 [cited 2020 May 5];34(16–17):1157–65. Available from: http://www.ncbi.nlm.nih.gov/pubmed/9566763
20. Kochenderfer JN, Yu Z, Frasheri D, Restifo NP, Rosenberg SA. Adoptive transfer of syngeneic T cells transduced with a chimeric antigen receptor that recognizes murine CD19 can eradicate lymphoma and normal B cells. Blood [Internet]. 2010 Nov 11 [cited 2020 Apr 22];116(19):3875–86. Available from: http://www.ncbi.nlm.nih.gov/pubmed/20631379
21. Huster KM, Koffler M, Stemberger C, Schiemann M, Wagner H, Busch DH. Unidirectional development of CD8+ central memory T cells into protective Listeria-specific effector memory T cells. Eur J Immunol [Internet]. 2006 Jun;36(6):1453–64. Available from: http://www.ncbi.nlm.nih.gov/pubmed/16637009
22. Bachmann MF, Wolint P, Schwarz K, Jäger P, Oxenius A. Functional properties and lineage relationship of CD8+ T cell subsets identified by expression of IL-7 receptor alpha and CD62L. J Immunol [Internet]. 2005 Oct 1;175(7):4686–96. Available from: http://www.ncbi.nlm.nih.gov/pubmed/16177116
23. Pietersz GA, Wenjun L, Sutton VR, Burgess J, McKenzie IF, Zola H, Trapani JA. In vitro and in vivo antitumor activity of a chimeric anti-CD19 antibody. Cancer Immunol Immunother [Internet]. 1995 Jul;41(1):53–60. Available from: http://www.ncbi.nlm.nih.gov/pubmed/7543822
24. Kochenderfer JN, Feldman SA, Zhao Y, Xu H, Black MA, Morgan RA, Wilson WH, Rosenberg SA. Construction and preclinical evaluation of an anti-CD19 chimeric antigen receptor. J Immunother [Internet]. 2009 Sep;32(7):689–702. Available from: http://www.ncbi.nlm.nih.gov/pubmed/19561539
25. Qin L, Lai Y, Zhao R, Wei X, Weng J, Lai P, Li B, Lin S, Wang S, Wu Q, Liang Q, Li Y, Zhang X, Wu Y, Liu P, Yao Y, Pei D, Du X, Li P. Incorporation of a hinge domain improves the expansion of chimeric antigen receptor T cells. J Hematol Oncol [Internet]. 2017;10(1):68. Available from: http://www.ncbi.nlm.nih.gov/pubmed/28288656
26. Rodgers DT, Mazagova M, Hampton EN, Cao Y, Ramadoss NS, Hardy IR, Schulman A, Du J, Wang F, Singer O, Ma J, Nunez V, Shen J, Woods AK, Wright TM, Schultz PG, Kim CH, Young TS. Switch-mediated activation and retargeting of CAR-T cells for B-cell malignancies. Proc Natl Acad Sci U S A [Internet]. 2016 Jan 26;113(4):E459-68. Available from: http://www.ncbi.nlm.nih.gov/pubmed/26759369
27. Sommermeyer D, Hudecek M, Kosasih PL, Gogishvili T, Maloney DG, Turtle CJ, Riddell SR. Chimeric antigen receptor-modified T cells derived from defined CD8+ and CD4+ subsets confer superior antitumor reactivity in vivo. Leukemia [Internet]. 2016 Feb;30(2):492–500. Available from: http://www.ncbi.nlm.nih.gov/pubmed/26369987
28. Klesmith JR, Wu L, Lobb RR, Rennert PD, Hackel BJ. Fine Epitope Mapping of the CD19 Extracellular Domain Promotes Design. Biochemistry [Internet]. 2019;58(48):4869–81. Available from: http://www.ncbi.nlm.nih.gov/pubmed/31702909
29. Baumann JG, Unutmaz D, Miller MD, Breun SKJ, Grill SM, Mirro J, Littman DR, Rein A, KewalRamani VN. Murine T Cells Potently Restrict Human Immunodeficiency Virus Infection. J Virol. 2004 Nov 15;78(22):12537–47.
30. Kerkar SP, Sanchez-Perez L, Yang S, Borman Z a, Muranski P, Ji Y, Chinnasamy D, Kaiser ADM, Hinrichs CS, Klebanoff C a, Scott CD, Gattinoni L, Morgan R a, Rosenberg S a, Restifo NP. GeneticKerkar, S. P., Sanchez-Perez, L., Yang, S., Borman, Z. a, Muranski, P., Ji, Y., … Restifo, N. P. (2011). Genetic engineering of murine CD8+ and CD4+ T cells for preclinical adoptive immunotherapy studies. Journal of Immunotherapy (Hagerstown, Md.□: J Immunother [Internet]. 2011 May [cited 2020 May 4];34(4):343–52. Available from: http://www.ncbi.nlm.nih.gov/pubmed/21499127
31. Tsurutani N, Yasuda J, Yamamoto N, Choi B-I, Kadoki M, Iwakura Y. Nuclear Import of the Preintegration Complex Is Blocked upon Infection by Human Immunodeficiency Virus Type 1 in Mouse Cells. J Virol. 2007 Jan 15;81(2):677–88.
32. Delville M, Soheili T, Bellier F, Durand A, Denis A, Lagresle-Peyrou C, Cavazzana M, Andre-Schmutz I, Six E. A Nontoxic Transduction Enhancer Enables Highly Efficient Lentiviral Transduction of Primary Murine T Cells and Hematopoietic Stem Cells. Mol Ther - Methods Clin Dev. 2018 Sep 21;10:341–7.
33. Follenzi A, Battaglia M, Lombardo A, Annoni A, Roncarolo MG, Naldini L. Targeting lentiviral vector expression to hepatocytes limits transgene-specific immune response and establishes long-term expression of human antihemophilic factor IX in mice. Blood [Internet]. 2004 May 15;103(10):3700–9. Available from: http://www.ncbi.nlm.nih.gov/pubmed/14701690
34. Pan D, Gunther R, Duan W, Wendell S, Kaemmerer W, Kafri T, Verma IM, Whitley CB. Biodistribution and toxicity studies of VSVG-pseudotyped lentiviral vector after intravenous administration in mice with the observation of in vivo transduction of bone marrow. Mol Ther [Internet]. 2002 Jul;6(1):19–29. Available from: http://www.ncbi.nlm.nih.gov/pubmed/12095299
35. Amirache F, Lévy C, Costa C, Mangeot P-E, Torbett BE, Wang CX, Nègre D, Cosset F-L, Verhoeyen E. Mystery solved: VSV-G-LVs do not allow efficient gene transfer into unstimulated T cells, B cells, and HSCs because they lack the LDL receptor. Blood [Internet]. 2014 Feb 27;123(9):1422–4. Available from: http://www.ncbi.nlm.nih.gov/pubmed/24578496
36. DePolo NJ, Reed JD, Sheridan PL, Townsend K, Sauter SL, Jolly DJ, Dubensky TW. VSV-G pseudotyped lentiviral vector particles produced in human cells are inactivated by human serum. Mol Ther [Internet]. 2000 Sep;2(3):218–22. Available from: http://www.ncbi.nlm.nih.gov/pubmed/10985952
37. Ruella M, Xu J, Barrett DM, Fraietta JA, Reich TJ, Ambrose DE, Klichinsky M, Shestova O, Patel PR, Kulikovskaya I, Nazimuddin F, Bhoj VG, Orlando EJ, Fry TJ, Bitter H, Maude SL, Levine BL, Nobles CL, Bushman FD, Young RM, Scholler J, Gill SI, June CH, Grupp SA, Lacey SF, Melenhorst JJ. Induction of resistance to chimeric antigen receptor T cell therapy by transduction of a single leukemic B cell. Nat Med [Internet]. 2018 Oct 1 [cited 2020 Apr 22];24(10):1499–503. Available from: http://www.ncbi.nlm.nih.gov/pubmed/30275568
38. Turtle CJ, Hanafi L-AA, Berger C, Gooley TA, Cherian S, Hudecek M, Sommermeyer D, Melville K, Pender B, Budiarto TM, Robinson E, Steevens NN, Chaney C, Soma L, Chen X, Yeung C, Wood B, Li D, Cao J, Heimfeld S, Jensen MC, Riddell SR, Maloney DG. CD19 CAR-T cells of defined CD4+:CD8+ composition in adult B cell ALL patients. J Clin Invest [Internet]. 2016 Jun 1 [cited 2020 Apr

22];126(6):2123–38. Available from: http://www.ncbi.nlm.nih.gov/pubmed/27111235
39. Braun CJ, Boztug K, Paruzynski A, Witzel M, Schwarzer A, Rothe M, Modlich U, Beier R, Göhring G, Steinemann D, Fronza R, Ball CR, Haemmerle R, Naundorf S, Kühlcke K, Rose M, Fraser C, Mathias L, Ferrari R, Abboud MR, Al-Herz W, Kondratenko I, Maródi L, Glimm H, Schlegelberger B, Schambach A, Albert MH, Schmidt M, von Kalle C, Klein C. Gene therapy for Wiskott-Aldrich syndrome--long-term efficacy and genotoxicity. Sci Transl Med [Internet]. 2014 Mar 12;6(227):227ra33. Available from: http://www.ncbi.nlm.nih.gov/pubmed/24622513
40. Hacein-Bey-Abina S, Garrigue A, Wang GP, Soulier J, Lim A, Morillon E, Clappier E, Caccavelli L, Delabesse E, Beldjord K, Asnafi V, MacIntyre E, Dal Cortivo L, Radford I, Brousse N, Sigaux F, Moshous D, Hauer J, Borkhardt A, Belohradsky BH, Wintergerst U, Velez MC, Leiva L, Sorensen R, Wulffraat N, Blanche S, Bushman FD, Fischer A, Cavazzana-Calvo M. Insertional oncogenesis in 4 patients after retrovirus-mediated gene therapy of SCID-X1. J Clin Invest [Internet]. 2008 Sep;118(9):3132–42. Available from: http://www.ncbi.nlm.nih.gov/pubmed/18688285
41. Howe SJ, Mansour MR, Schwarzwaelder K, Bartholomae C, Hubank M, Kempski H, Brugman MH, Pike-Overzet K, Chatters SJ, de Ridder D, Gilmour KC, Adams S, Thornhill SI, Parsley KL, Staal FJT, Gale RE, Linch DC, Bayford J, Brown L, Quaye M, Kinnon C, Ancliff P, Webb DK, Schmidt M, von Kalle C, Gaspar HB, Thrasher AJ. Insertional mutagenesis combined with acquired somatic mutations causes leukemogenesis following gene therapy of SCID-X1 patients. J Clin Invest [Internet]. 2008 Sep;118(9):3143–50. Available from: http://www.ncbi.nlm.nih.gov/pubmed/18688286
42. Ott MG, Schmidt M, Schwarzwaelder K, Stein S, Siler U, Koehl U, Glimm H, Kühlcke K, Schilz A, Kunkel H, Naundorf S, Brinkmann A, Deichmann A, Fischer M, Ball C, Pilz I, Dunbar C, Du Y, Jenkins NA, Copeland NG, Lüthi U, Hassan M, Thrasher AJ, Hoelzer D, von Kalle C, Seger R, Grez M. Correction of X-linked chronic granulomatous disease by gene therapy, augmented by insertional activation of MDS1-EVI1, PRDM16 or SETBP1. Nat Med [Internet]. 2006 Apr;12(4):401–9. Available from: http://www.ncbi.nlm.nih.gov/pubmed/16582916
43. Raper SE, Chirmule N, Lee FS, Wivel NA, Bagg A, Gao G, Wilson JM, Batshaw ML. Fatal systemic inflammatory response syndrome in a ornithine transcarbamylase deficient patient following adenoviral gene transfer. Mol Genet Metab [Internet]. 80(1–2):148–58. Available from: http://www.ncbi.nlm.nih.gov/pubmed/14567964
44. Stein S, Ott MG, Schultze-Strasser S, Jauch A, Burwinkel B, Kinner A, Schmidt M, Krämer A, Schwäble J, Glimm H, Koehl U, Preiss C, Ball C, Martin H, Göhring G, Schwarzwaelder K, Hofmann W-K, Karakaya K, Tchatchou S, Yang R, Reinecke P, Kühlcke K, Schlegelberger B, Thrasher AJ, Hoelzer D, Seger R, von Kalle C, Grez M. Genomic instability and myelodysplasia with monosomy 7 consequent to EVI1 activation after gene therapy for chronic granulomatous disease. Nat Med [Internet]. 2010 Feb;16(2):198–204. Available from: http://www.ncbi.nlm.nih.gov/pubmed/20098431
45. Booth C, Gaspar HB, Thrasher AJ. Treating Immunodeficiency through HSC Gene Therapy. Trends Mol Med [Internet]. 2016 Apr;22(4):317–27. Available from: http://www.ncbi.nlm.nih.gov/pubmed/26993219
46. Milone MC, O'Doherty U. Clinical use of lentiviral vectors. Leukemia [Internet]. 2018;32(7):1529–41. Available from: http://www.ncbi.nlm.nih.gov/pubmed/29654266
47. Cornetta K, Duffy L, Turtle CJ, Jensen M, Forman S, Binder-Scholl G, Fry T, Chew A, Maloney DG, June CH. Absence of Replication-Competent Lentivirus in the Clinic: Analysis of Infused T Cell Products. Mol Ther [Internet]. 2018 Jan 3 [cited 2020 May 4];26(1):280–8. Available from: http://www.ncbi.nlm.nih.gov/pubmed/28970045
48. Marcucci KT, Jadlowsky JK, Hwang WT, Suhoski-Davis M, Gonzalez VE, Kulikovskaya I, Gupta M, Lacey SF, Plesa G, Chew A, Melenhorst JJ, Levine BL, June CH. Retroviral and Lentiviral Safety Analysis of Gene-Modified T Cell Products and Infused HIV and Oncology Patients. Mol Ther. 2018 Jan 3;26(1):269–79.
49. Turtle CJ, Hanafi L-A, Berger C, Gooley TA, Cherian S, Hudecek M, Sommermeyer D, Melville K, Pender B, Budiarto TM, Robinson E, Steevens NN, Chaney C, Soma L, Chen X, Yeung C, Wood B, Li D, Cao J, Heimfeld S, Jensen MC, Riddell SR, Maloney DG. CD19 CAR-T cells of defined CD4+:CD8+ composition in adult B cell ALL patients. J Clin Invest [Internet]. 2016;126(6):2123–38. Available from: http://www.ncbi.nlm.nih.gov/pubmed/27111235
50. Zufferey R, Nagy D, Mandel RJ, Naldini L, Trono D. Multiply attenuated lentiviral vector achieves efficient gene delivery in vivo. Nat Biotechnol. 1997;15(9):871–5.
51. Naldini L, Blömer U, Gallay P, Ory D, Mulligan R, Gage FH, Verma IM, Trono D. In vivo gene delivery and stable transduction of nondividing cells by a lentiviral vector. Science (80-). 1996 Apr 12;272(5259):263–7.
52. Dull T, Zufferey R, Kelly M, Mandel RJ, Nguyen M, Trono D, Naldini L. A third-generation lentivirus vector with a conditional packaging system. J Virol [Internet]. 1998 Nov [cited 2020 Apr 22];72(11):8463–71. Available from: http://www.ncbi.nlm.nih.gov/pubmed/9765382

Figures

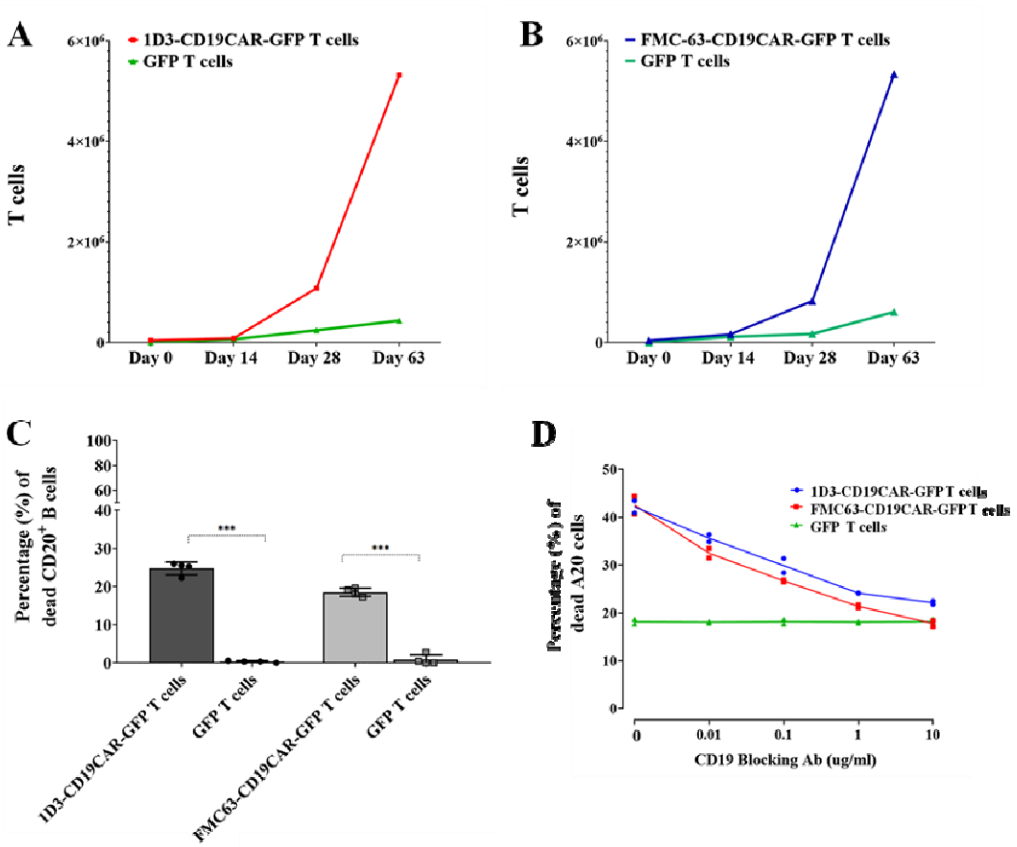

Figure 1: ***In vitro* proliferation and cytolytic activity of murine CAR-T cells. Figure 1A**: $2.5x10^5$ C57BL/6 splenocytes were transduced with 1D3-CD19CAR-GFP or GFP-only lentivirus at an MOI of 5. The transduced splenocytes were then co-cultured with an excess of irradiated C57BL/6 splenocytes which provided a source of B cells expressing the CD19 antigen. The 1D3-CD19CAR transduced splenocytes showed a 12.2+/- 0.09 (mean +/- SD) fold expansion (red, square), compared to GFP transduced (green, triangle) ($p < 0.002$ paired, two-tail T test). **Figure 1B**: $2.5x10^5$ C57BL/6 splenocytes were transduced with the FMC63-CD19CAR-GFP or GFP-only lentivirus at an MOI of 5. Splenocytes were then co-cultured with irradiated C57BL/6 splenocytes which provided a source of B cells expressing the CD19 antigen. The FMC63-CD19CAR transduced splenocytes showed a 8.8 +/- 0.03 fold expansion (orange, square), compared to GFP transduced (cyan, triangle), ($p < 0.004$ paired, two-tail T test). **Figure 1C**: $1x10^5$ FMC63-CD19CAR-GFP or 1D3-CD19CAR murine T cells from day 63 of the expansion assays were co-cultured for 5 hours with target B cells, isolated from C57BL/6 splenocytes, at a E:T ratio of 1:1. Unviable target murine B cells were measured through the shift in the FVS780 signal, measured by flow cytometry [**Figure S4**]. Expanded murine 1D3-CAR-T cells showed robust and selective targeting of murine B cells, with 24.8 +/- 1.69% of B cells being unviable after a 5 hour co-culture. The FMC63-CD19CAR T cells also showed robust and selective targeting of murine B cells with 18.5 +/- 1.08 % of B cells being unviable after a 5 hour co-culture.. Two-way ANOVA, Sidak's multiple comparison ***$p<0.002$. **Figure 1D**: 1D3-, FMC63-CD19CAR, and GFP- transduced and expanded murine T cells were co-cultured with target A20 cells for 4 hours. The CD19 antigen on the A20 cells, were blocked with either the CD19 -1D3 or -FMC63 blocking antibody at a starting concentration of 10µg/ml decreasing 10 fold down to 0µg/ml, at an E:T ratio of 4:1. Using flow cytometry, target cell death was measured through the shift in the FVS780 signal, [**Figure S3** and **Table S1**]. The murine CAR-T cells showed robust and selective response when co-cultured with A20 cells. This response decreased with increasing CD19 blocking antibody concentration. 38.8+/- 0.71% of unblocked A20 cells were unviable when co-cultured with the 1D3-CD19CAR T cells, which decreased to 19.7 +/-0.28% of A20 cells blocked with 10µg/ml of 1D3-CD19 blocking antibody. 41.1+/- 0.92% of unblocked A20 cells were unviable when co-cultured with the FMC63-CD19CAR T cells, which decreased to 20.8 +/-0.57% of A20 cells blocked with 10µg/ml of FMC63-CD19 blocking. Two-way ANOVA $p = 0.04$. Nonlinear regression analysis (Sigmoidal) analysis of 1D3-CD19CAR T cells vs A20 CD19 blocking antibody dose response, R^2 =0.95. FMC63- CD19CAR T cells vs A20 CD19 blocking antibody dose response, R^2 = 0.96. GFP vs A20 CD19 blocking antibody dose response, R^2 =0.01.

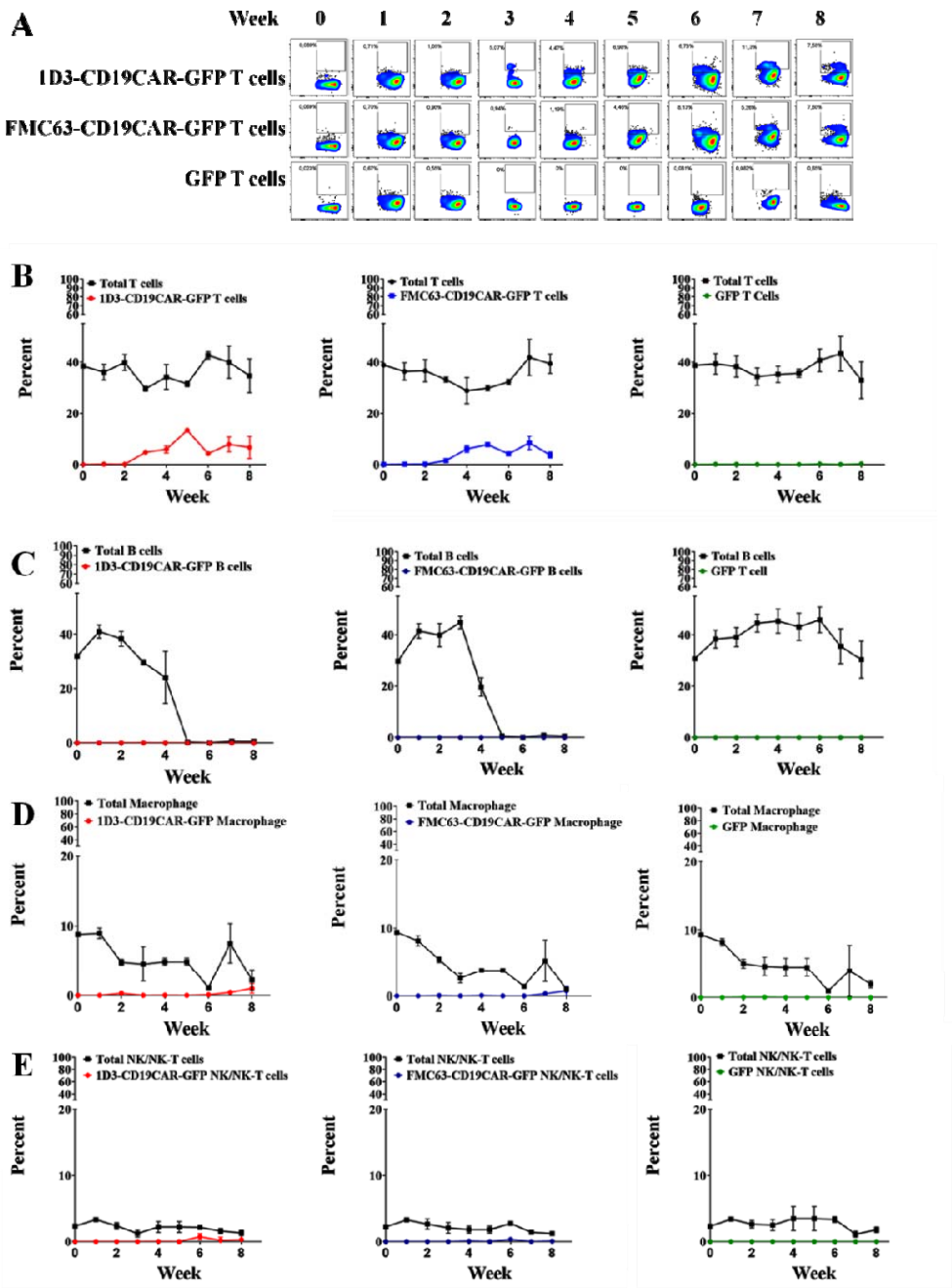

Figure 2: The abundance of immune cell subsets in treated mice over time, as a percent of total PBMC. C57BL/6 wildtype mice were treated with a single IV injection of lentivirus (3.6-4.0 x10^6 IU in 200µl PBS), to deliver either the 1D3-CD19CAR-GFP CAR, FMC63-CD19 CAR, or control (GFP-only) N equals 8 mice per group and error bars represent the standard deviation from the mean value reported for each group. T cells, but not other immune cell subsets tested, show a substantial transduced cell population. **Figure 2A**: Representative flowgrams showing increasing GFP positive T cells in PBMC of treated mice, over time. The X-axis of the flowgrams is CD3 positivity and GFP positivity on the Y-axis. from **Figure 2B-2E**. **Figure 2B**: Total T cells versus 1D3-, FMC63-CD19CAR, and GFP transduced T cells ($CD3^+$, $CD90.2^+$ T cells). **Figure 2C**: Total B cells versus 1D3-, FMC63-CD19CAR, and GFP transduced B cells ($CD20^+$, $CD45R/B220^+$ B cells). **Figure 2D:** Total macrophage versus 1D3-, FMC63-CD19CAR, and GFP transduced macrophage ($CD11b^+$ macrophage and other non-T cells). **Figure 2E**: Total NK/NK-T cells versus 1D3-, FMC63-CD19CAR, and GFP transduced NK/NK-T cells ($CD335^+$ NK / NKT cells). Flow gating strategy outlined in **Figure S4** and data in **Table S3 and Table S4**.

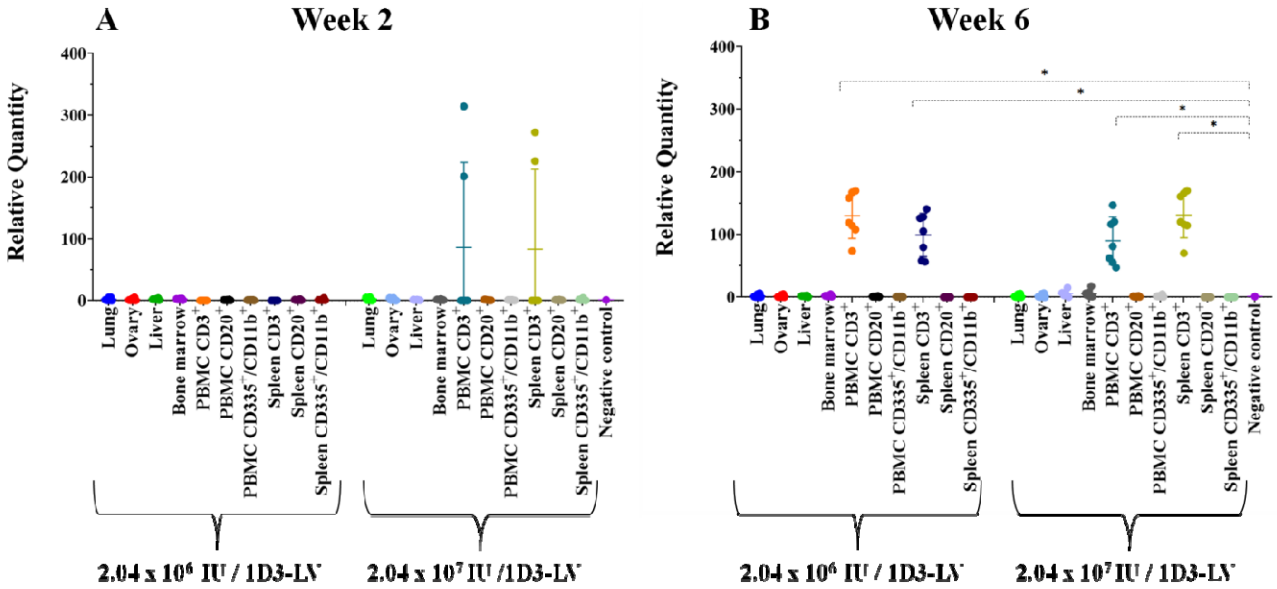

Figure 3: Quantitative PCR analysis of transgene positivity. DNA from $CD3^+$, $CD20^+$, and $CD355^+/11b^+$ cells, sorted from PBMC and spleen samples and from liver, lung, bone marrow, and the ovaries was obtained from female C57BL/6 mice. N equals 7 mice per group and the error bars represent the standard deviation from the mean value reported for each group. [**Figure 3A**] 2 weeks and [**Figure 3B**] 6 weeks after being treated with $2.04x10^6$ or $2.04x10^7$ IU of the 1D3-CD19CAR lentivirus, respectively. The 1D3-CD19CAR-GFP transgene were prominent only in the $CD3^+$ T cell populations isolated from both PBMC and spleens 6 weeks posts 1D3-CD19CAR-LV treatment (**Figure 3B**. Orange 132.7 +/- 27.77, dark blue 131.0 +/- 35.42, cyan 129.9 +/- 34.75, and mustard 147.1 +/- 41.42). Relative quantity was calculated using the ΔΔCT calculation using the murine reference gene β-actin and unmodified C57BL/6 spleen cells as the reference control.We also see evidence of CD19CAR-T possession at week 2, in $CD3^+$ T cells isolated from the spleen and PBMCs of two (2) mice which received 2.04 x 10^7 IU of the 1D3-CD19CAR-LV (**Figure 3A**; cyan and mustard). **Figure 3A;** ANOVA ***p <0.001, **Figure 3B;** ANOVA***p <0.001. Using Dunnett's post-hoc analysis, comparing PBMC and spleen T cells, 6 weeks after treatment with 2.04 x 10^6 of the 1D3-CD19CAR-LV with the negative control, * p > 0.015.

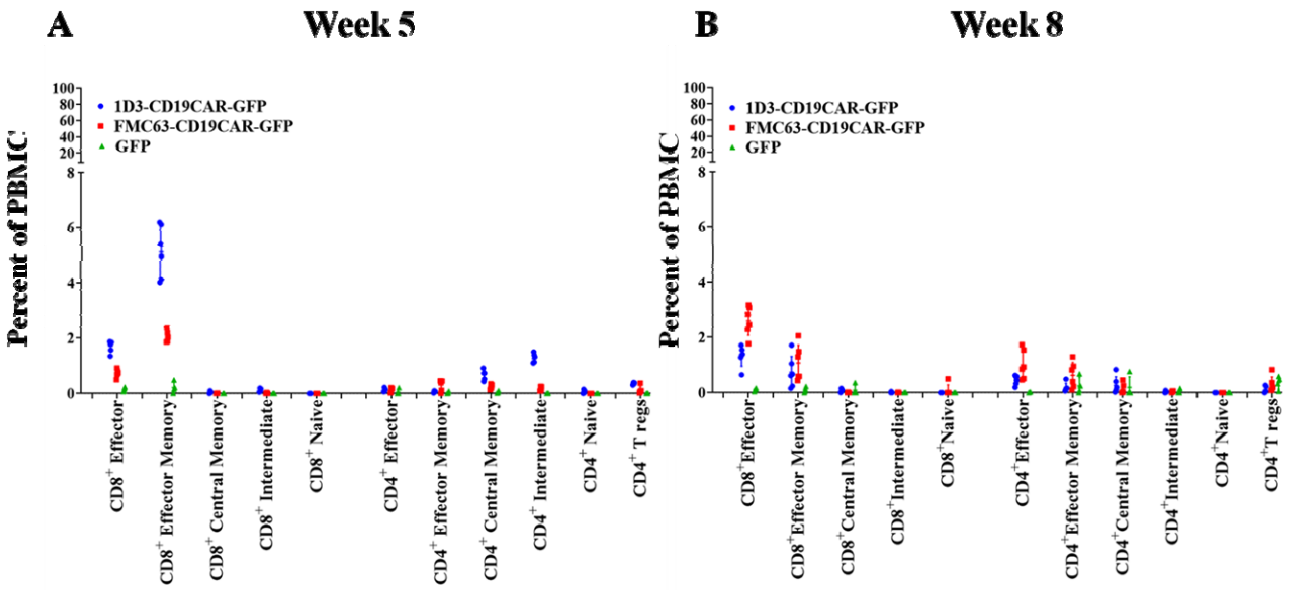

Figure 4: Immunophenotyping of 1D3-CD19CAR-GFP (blue, circle), FMC63-CD19 CAR-GFP (red, square) or control (GFP-only, green, triangle) transduced T cells in peripheral blood of treated mice. Values shown are the percentage of total $CD3^+$, $CD90.2^+$ T cells represented by each subtype (Effector = $CD44^{high}$, $CD62L^{low}$ $CD127^{low}$; effector memory = $CD44^{high}$, $CD62L^{low}$ $CD127^{high}$; central memory = $CD44^{high}$, $CD62L^{high}$ $CD127^{high}$; intermediate phenotype = $CD44^{high}$ $CD62L^{high}$ $CD127^{low}$; naive = $CD44^{low}$, $CD62L^{high}$ $CD127^{high}$; regulatory = $CD4^+FOXP3^+$). N equals 8 mice per group and error bars represent the standard deviation from the mean value reported for each group. **Figure 4A**: At week 5 the 1D3-CD19CAR-GFP T cells were predominantly $CD8^+$ effector memory T cells (5.1 +/- 0.9% of total $CD3^+$ T cells), effector T cells (1.7 +/- 0.2% of total $CD3^+$ T cells), and $CD4^+$ intermediate T cells (1.3 +/- 0.2% of total $CD3^+$ T cells). At week 5 the majority of FMC63-CD19CAR-GFP T cells were $CD8^+$ effector memory T cells (2.0 +/- 0.2% of total $CD3^+$ T cells) and effector T cells (0.7 +/- 0.1% of total $CD3^+$ T cells). **Figure 4B**: At week 8, the majority of 1D3-CD19CAR-GFP T cells were effector memory T cells (0.7 +/- 0.6% of total $CD3^+$ T cells) and $CD8^+$ effector T cells (1.3+/- 0.4% of total $CD3^+$ T cells). The majority of FMC63-CD19CAR-GFP T cells at week 8 were $CD8^+$ effector memory T cells (2.60 +/- 0.538% of total $CD3^+$ T cells) and effector T cells (1.1 +/- 0.6% of total $CD3^+$ T cells). GFP expressing $CD4^+$ $FOXP3^+$ regulator T cells were present at both time points but comprised of a small percentage (<1%) of total T cells. Flow gating strategy outlined in **Figure S5** and data in **Table S5**.

Supplementary Materials

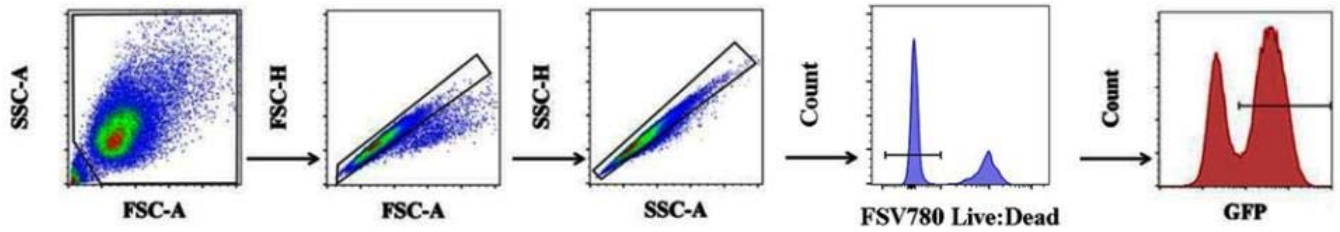

Figure S1: Viral supernatant titration flow gating protocol. After debris was eliminated by FSC-A vs. SSC-A gating, cell doublets and clumps were then eliminated by FSC-H vs. FSC-A gating followed by SSC-A vs. SSC-H gating. The live cells were determined by gating on the FVS780 negative cells and then the GFP positive cells were determined to establish the percentage of GFP expressing cells in order to measure transduction efficiency. The flow collected data was analysed using Flow Jo v10, for windows and GraphPad Prism software version 8.0.0 for windows (GraphPad Software, California, USA).

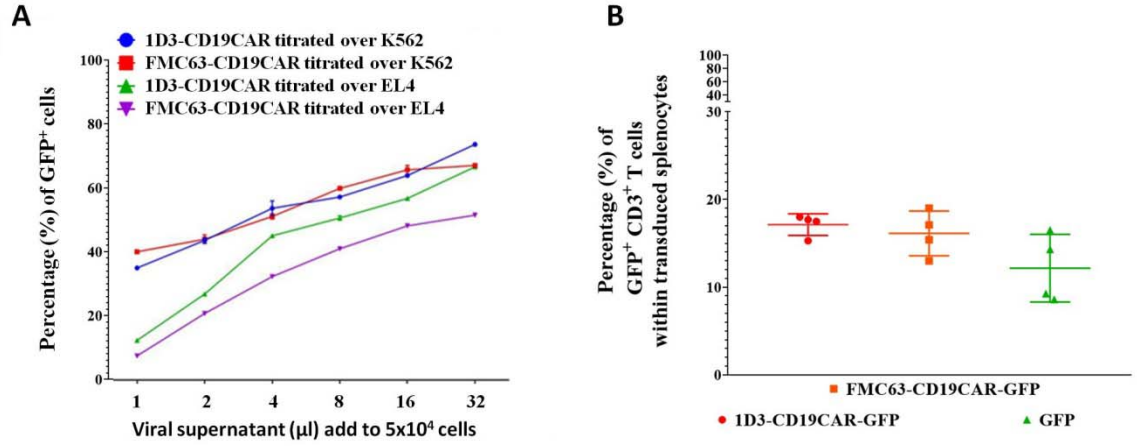

Figure S2: 1D3-CD19CAR-GFP, FMC63-CD19CAR-GFP, and GFP lentivirus transduction efficiency. **Figure S2A**: Titration of 1D3- CD19CAR-GFP and FMC63-CD19CAR-GFP viral supernatant titration over EL4 (green and purple, respectively) and K562 (red and blue, respectively) cell lines. While the transduction efficiency appears significantly better in the human K562s ($p < 0.001$ ANOVA), the transduction of a murine cell line, EL4, indicates this lentivirus is able to transduce murine cells, albeit at a lower frequency. **Figure S2B**: $2.5x10^5$ splenocytes were transduced with 1D3-CD19CAR-GFP, FMC63-CD19CAR-GFP, and GFP lentivirus at an MOI of 5 (calculated based on Figure S2A). The percentage (%) of GFP^+, CD3+ T cells within the whole splenocyte sample was determined by assessing $3.0x10^4$ cells via flow cytometry 72 hours after transduction with virus. 1D3-CD19CAR-GFP had a transduction efficiency of 17.1% (+/-1.23%), FMC63-CD19CAR-GFP 16.3% (+/- 2.6%), and GFP 12.2% (+/- 3.85%).

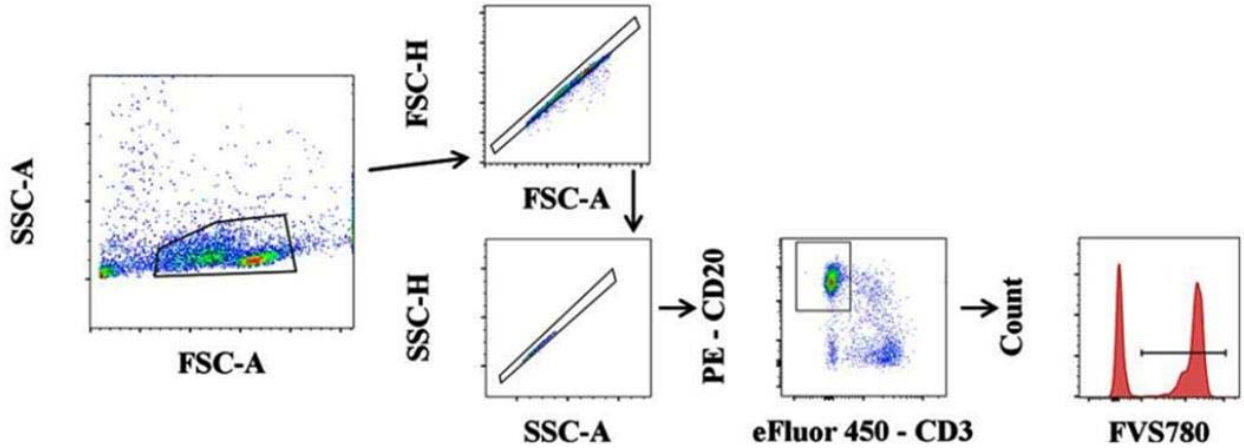

Figure S3: *In vitro* 1D3- or FMC63-CD19CAR-GFP T cell cytolytic activity using C57BL/6 splenocytes and A20 cells blocked with serially diluted concentrations of CD19 blocking antibodies. Debris, cell doublets, and clumps were eliminated by FCS-A vs SSC-A gating followed by FSC-A vs. FSC-H and SSC-A vs. SSC-H gating. T and B cells were then identified by CD3 vs. CD20 gating. CD20 positive cells were selected for and gated on FVS-780 to obtain the percentage of live vs. dead target cells. The flow collected data was analysed using Flow Jo v10, for windows and GraphPad Prism software version 8.0.0 for windows (GraphPad Software, California, USA) [**Figure 1**]

Table S1: Cell numbers for the *In vitro* 1D3- or FMC63-CD19CAR-GFP T cell cytolytic activity using C57BL/6 splenocytes data showed in **Figure 1C** and **Figure S3**

	1D3-CD19CAR-GFP		**FMC63-CD19CAR-GFP**	
	Mean cell count	**SD**	**Mean cell count**	**SD**
CD19CAR-GFP	12387	845.6	9263	540.6
GFP	167	120.1	400	658.6

Table S2: Cell numbers for the *In vitro* 1D3- or FMC63-CD19CAR-GFP T cell cytolytic activity using A20 cells blocked with serially diluted concentrations of CD19 blocking antibodies data showed in **Figure 1D** and **Figure S3.**

Blocking Ab (µg/ml)	**1D3-CD19CAR-GFP**		**FMC63-CD19CAR-GFP**		**GFP**	
	Mean cell count	**SD**	**Mean cell count**	**SD**	**Mean cell count**	**SD**
0.00	19400	353.6	20525	459.6	9100	353.6
0.01	17000	636.4	17425	247.5	9025	106.1
0.10	14050	212.1	14100	495.0	9100	353.6
1.00	11400	282.8	10950	565.7	9025	106.1
10.0	9850	141.4	10400	282.8	9100	353.64

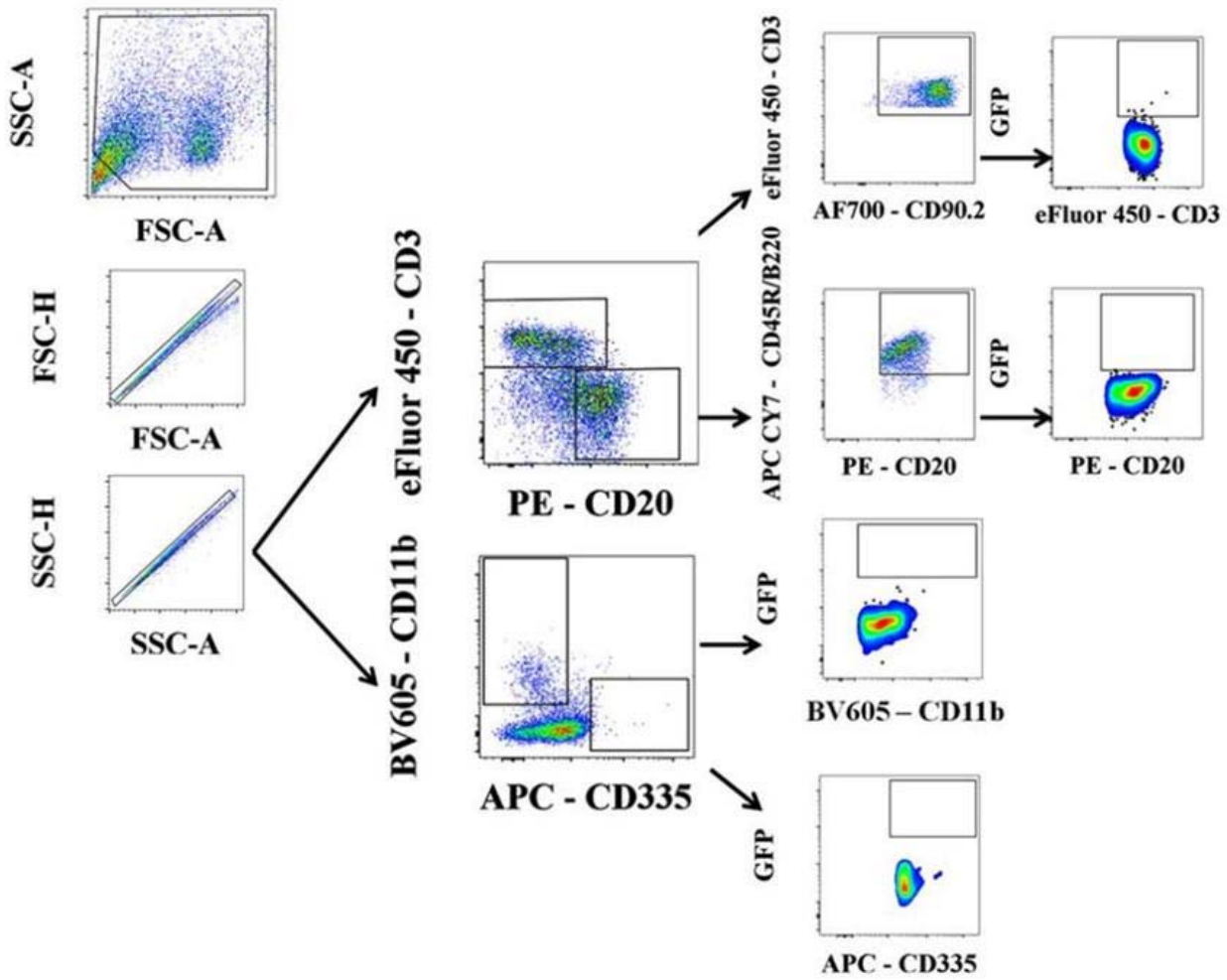

Figure S4: Flow gating protocol for the analysis of mouse blood pre- and post-treatment with lentiviruses. Debris was eliminated by FSC-A vs. SSC-A gating, cell doublets and clumps were then eliminated by FSC-H vs. FSC-A gating followed by SSC-A vs. SSC-H gating. T and B cells were then identified based on expression of CD3 or CD20 and NK cells and monocytes based on the expression of CD335 or CD11b, respectively. The CD3 positive cells were then gated for expression of CD90.2, and these CD3 and CD90.2 positive cells were gated for GFP expression (the CD19CAR reference gene marker). CD20 positive cells were gated for CD45R/B220 expression, and the CD20 and CD45R/B220 positive cells were then gated for GFP expression. NK cells (CD335) or monocytes (CD11b) were individually gated for GFP expression. The flow collected data was analysed using Flow Jo v10, for windows and GraphPad Prism software version 8.0.0 for windows (GraphPad Software, California, USA) [**Figure 2**]

Table S3: Cell numbers for B and T cells from flow cytometry data collected in the *in vivo* experiments, shown in **Figure 2** and **Figure 3** and flow gating protocol shown in **Figure S5**

		GFP+ B cells		B cells		GFP+ T cells		T cells	
	Week	**Mean cell count**	**SD**	**Mean cell count**	**SD**	**Mean cell count**	**SD**	**Mean cell count**	**SD**
1D3-CD19CAR-GFP	0	4	6.13	15943	101.8	6	5.8	19214	140.6
	1	1	3.6	20479	1220.3	84	42.48	18043	1511.7
	2	2	5.1	19128	1382.0	53	17.68	19943	1567.8
	3	23	39.5	14807	474.7	2421	255.6	14807	474.7
	4	0	0	12043	4772.6	2973	711.8	17100	2409.7
	5	0	0	144	32.3	6707	290.7	15764	536.0
	6	0	0	20	13.3	2166	124.3	21329	722.2
	7	0	0	294	77.2	3944	1446.1	20014	3161.9
	8	0	0	275	96.9	3346	2163.8	17329	3298.9
FMC63-CD19CAR-GFP	0	0	0	14883	169.3	17	14.1	19425	181.0
	1	12	18.83	20767	1423.6	67	19.7	18183	1702.3
	2	3	7.3	19933	2273.0	75	18.4	18317	2166.7
	3	10	24.5	22425	1221.0	775	84.7	16575	504.7
	4	0	0	9833	1792.3	3061	655.6	14433	2556.3
	5	0	0	281	281.1	3890	378.9	14925	503.7
	6	0	0	46	20.4	2099	158.9	16133	503.7
	7	0	0	429	56.3	4239	1345.0	20925	3533.8
	8	0	0	255	49.2	1880	575.0	19700	1882.0
GFP	0	2	5.0	15343	395.2	14	22.3	19357	185.8
	1	3	5.5	19157	1745.1	66	36.8	19671	2002.7
	2	11	12.4	19550	1869.5	59	22.8	19150	2076.7
	3	0	0	22279	1749.0	29	18.1	17179	1689.6
	4	0	0	22679	2342.3	15	18.8	17614	1581.1
	5	0	0	21571	2655.3	35	35.8	17850	798.4
	6	0	0	22928	2501.0	116	42.4	20364	2216.0
	7	15	22.8	17776	3410.6	33	11.7	21636	34
	8	13	5.8	15157	3602.4	129	66.1	16471	3576.3

Table S4: Cell numbers for CD335^{+} and CD11b^{+} cells from flow cytometry data collected in the *in vivo* experiments, shown in **Figure 2** and **Figure 3** and flow gating protocol shown in **Figure S5**

		GFP+ CD355 cells		**CD355 cells**		**GFP+ CD11b cells**		**CD11b cells**	
	Week	**Mean cell count**	**SD**	**Mean cell count**	**SD**	**Mean cell count**	**SD**	**Mean cell count**	**SD**
1D3-CD19CAR-GFP	0	0	0	1172	70.4	0	0	4392	62.4
	1	0	0	1661	102.7	0	0	4482	369.6
	2	0	0	1186	250.5	148	99.5	2402	216.2
	3	0	0	614	275.9	0	0	2487	537.2
	4	14	22.5	1104	407.8	14	22.5	2550	247.2
	5	0	0	1228	418.5	0	0	2441	261.2
	6	369	236.6	1076	50.2	44	117.2	556	24.7
	7	91	241.9	797	194.8	213	134.0	3769	1415.9
	8	140	370.4	659	211.9	496	343.6	1098	747.0
FMC63-CD19CAR-GFP	0	0	0	1118	37.0	0	0	4696	64.1
	1	0	0	1638	73.9	0	0	4075	375.5
	2	0	0	1324	385.6	33	53.3	2704	226.0
	3	0	0	1038	402.3	0	0	1303	351.6
	4	33	8.3	917	272.4	35	8.3	1772	110.4
	5	0	0	906	244.0	0	0	1887	139.5
	6	168	119.9	1371	80.8	0	0	699	34.6
	7	0	0	707	104.1	155	136.0	2597	1541.6
	8	34	83.7	612	80.4	366	346.4	479	46.4
GFP	0	0	0	1163	63.4	0	0	4639	105.9
	1	0	0	1694	69.7	0	0	4093	273.0
	2	0	0	1318	279.1	27	45.3	2512	328.8
	3	0	0	1246	413.2	26	32.7	2298	710.5
	4	0	0	1662	882.4	0	0	2114	623.5
	5	0	0	1737	904.0	0	0	2234	675.3
	6	0	0	1663	218.2	0	0	477	136.9
	7	0	0	558	232.3	0	0	1969	1886.9
	8	0	0	895	207.6	0	0	960	270.3

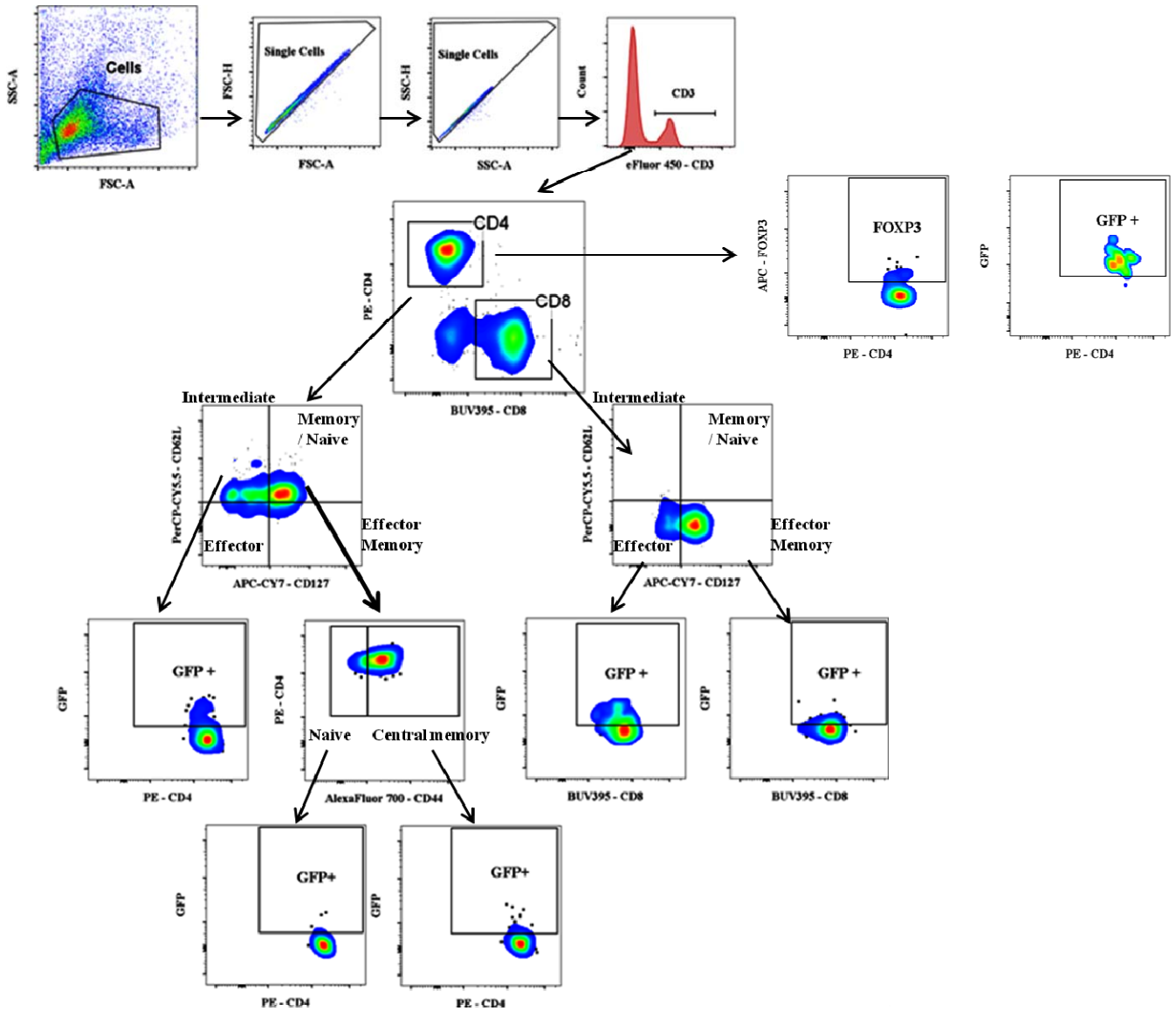

Figure S5: Flow gating protocol for the immunophenotyping analysis of murine T cells 5 and 8 weeks after lentiviral treatment. All cells were gated for in the FSC-A vs. SSC-A plot, cell doublets and clumps were then eliminated by FSC-H vs. FSC-A gating followed by SSC-A vs. SSC-H gating. T cells were then identified based on expression of CD3. The CD3 positive cells were then gated for expression of CD4 and CD8, and these $CD3^+$ and $CD8^+$ or $CD4^+$positive cells were gated for CD127 and CD62L expression, allowing us to differentiate Central memory and naive cells, effector, and effector memory T cells. The Central Memory and Naive cells were then identified by their CD44 expression profile. Each of these subtypes were then looked at for GFP expression (the CD19CAR reference gene marker) indicated by the example plots above showing the positive expression of GFP. For regulatory T cells we plotted the $CD4^+$ against the FOXP3, and then looked the number which expressed GFP. The flow collected data was analysed using Flow Jo v10, for windows and GraphPad Prism software version 8.0.0 for windows (GraphPad Software, California, USA) [**Figure 4**].

Table S5: Cell numbers for Immunophenotyping of 1D3-CD19CAR-GFP, FMC63-CD19 CAR-GFP, and GFP-only transduced T cells in peripheral blood of treated mice at week 5 and week 8 post treatment shown in **Figure 4** and flow gating protocol shown in **Figure S5**

		1D3-CD19CAR-GFP		**FMC63-CD19CAR-GFP**		**GFP**	
		Mean cell count	**SD**	**Mean cell count**	**SD**	**Mean cell count**	**SD**
Week 5	$CD8^+$Effector	1701	203.1	733	138.9	139	75.4
	$CD8^+$Effector Memory	5135	938.0	2029	205.0	215	203.4
	$CD8^+$Central Memory	42	34.6	8	8.5	2	4.25
	$CD8^+$Intermediate	109	58.9	7	13.6	0	0.0
	$CD8^+$Naive	0	0.0	0	0.0	0	0.0
	$CD4^+$Effector	121	61.5	131	77.3	53	105.0
	$CD4^+$Effector Memory	62	26.83	311	196.6	29	38.4
	$CD4^+$Central Memory	682	172.93	236	83.1	45	41.6
	$CD4^+$Intermediate	1262	164.3	154	76.5	3	6.4
	$CD4^+$Naive	55	57.2	0	0	0	0
	$CD4^+$T reg	355	32.7	118	128.3	3	6.4
Week 8	$CD8^+$Effector	1320	363.2	2604	538.3	110	52.5
	$CD8^+$Effector Memory	742	573.2	1075	637.5	98	99.0
	$CD8^+$Central Memory	71	52.2	3	6.8	91	182.5
	$CD8^+$Intermediate	10	16.3	4	4.8	4	7.25
	$CD8^+$Naive	2	2.5	83	204.1	0	0
	$CD4^+$Effector	460	169.3	1003	523.6	16	11.7
	$CD4^+$Effector Memory	186	155.4	634	465.3	252	304.0
	$CD4^+$Central Memory	270	309.2	127	190.0	191	382.5
	$CD4^+$Intermediate	25	31.0	38	25.1	39	77.5
	$CD4^+$Naive	1	2.2	0	0.0	0	0.0
	$CD4^+$T reg	102	114.8	289	283.3	362	234.8

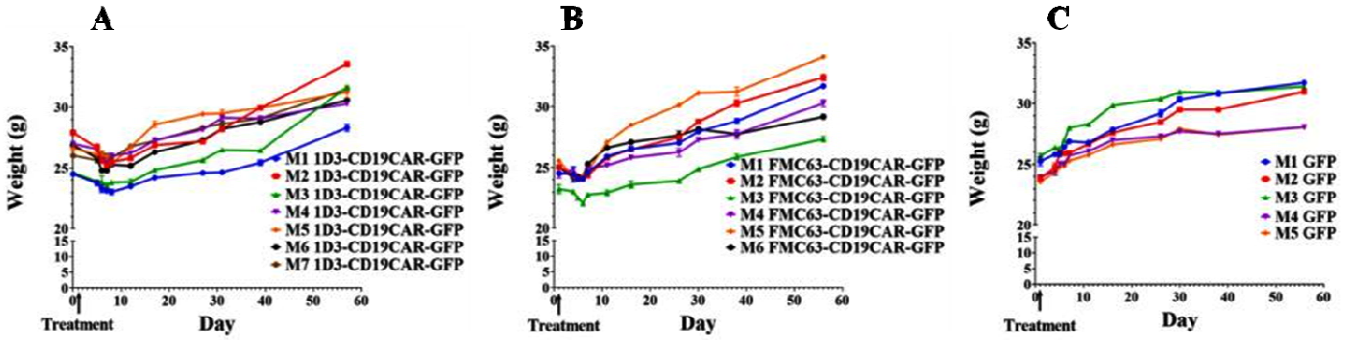

Figure S6: C57BL/6weights (grams) pre- and post treatment (n=8). Figure S6A: 1D3-CD19CAR-GFP lentivirus, Figure S6B: FMC63-CD19CAR-GFP lentivirus, and Figure S6C: GFP-only lentivirus or PBS. In **Figure S6A** and **S6B**, the mice that were treated with the 1D3-CD19CAR-GFP lentivirus or the FMC63-CD19CAR-GFP showed a 5.5 +/- 2.97% (mean +/- SD) and 3.6 +/- 1.78% reduction in weight, respectively, within 5-7 days after receiving treatment. Once the mice weights recovered, they exhibited no other visible adverse effects.

A

```
CLUSTAL 2.1 multiple sequence alignment


CD19_HUMAN      MPPPRLLFFLLFLTPMEVRPEEPLVVKVEEGDNAVLQCLKGTSDGPTQQLTWSRESPLKP 60
CD19_MOUSE      MPSPLPVSFLLFLTLVGGRPQKSLLVEVEEGGNVVLPCLPDSSPVSSEKLAWYRGNQSTP 60
                **.*  : ****** :  **:.*:*:****.*.** ** .:*  .:::*:* * .  .*

CD19_HUMAN      FLKLSLGLPGLGIHMRPLAIWLFIFNVSQQMGGFYLCQPGPPSEKAWQPGWTVNVEGSGE 120
CD19_MOUSE      FLELSPGSPGLGLHVGSLGILLVIVNVSDHMGGFYLCQKRPPFKDIWQPAWTVNVEDSGE 120
                **:** * ****:*: .*.* *.*.***::********  ** :. ***.******.***

                                                EEEEEEEEEEEEEEEEEE
CD19_HUMAN      LFRWNVSDLGGLGCGLKNRSSEGPSSPSGKLMSPKLYVWAKDRPEIWEGEPPCLPPRDSL 180
CD19_MOUSE      MFRWNASDVRDLDCDLRNRSSGSHRSTSG----SQLYVWAKDHPKVWGTKPVCAPRGSSL 176
                :****.**: .*.*.*:**** .  *.**    .:*******:*::*  :* * *  .**

CD19_HUMAN      NQSLS-QDLTMAPGSTLWLSCGVPPDSVSRGPLSWTHVHPKGP-KSLLSLELKDDRPARD 238
CD19_MOUSE      NQSLINQDLTVAPGSTLWLSCGVPPVPVAKGSISWTHVHPRRPNVSLLSLSLGGEHPVRE 236
                ****  ****:************** .*::*.:*******: *  *****.* .::*.*:

CD19_HUMAN      MWVMETGLLLPRATAQDAGKYYCHRGNLTMSFHLEITARPVLWHWLLRTGGWKVSAVTLA 298
CD19_MOUSE      MWVWGSLLLLPQATALDEGTYYCLRGNLTIERHVKVIARSAVWLWLLRTGGWIVPVVTLV 296
                ***  : ****:*** * *.*** *****:. *::: **..:* ******** *..***.

CD19_HUMAN      YLIFCLCSLVGILHLQRALVLRRKRKRMTDPTRRFFKVTPPPGSGPQNQYGNVLSLPTPT 358
CD19_MOUSE      YVIFCMVSLVAFLYCQRAFILRRKRKRMTDPARRFFKVTPPSGNGTQNQYGNVLSLPTST 356
                *:***: ***.:*: ***::***********:*********.*.*.************.*

CD19_HUMAN      SGLGRAQRWAAGLGGTAPSYGNPSSDVQADGALGSRSPPGVGPEEEEGEGYEEPDSEEDS 418
CD19_MOUSE      SGQAHAQRWAAGLGSVPGSYGNPRIQVQDTGAQSHETG-----LEEEGEAYEEPDSEEGS 411
                ** .:*********... *****  :**  ** . .:       *****.********.*

CD19_HUMAN      EFYENDSNLGQDQLSQDGSGYENPEDEPLGPEDEDSFSNAESYENEDEELTQPVARTMDF 478
CD19_MOUSE      EFYENDSNLGQDQVSQDGSGYENPEDEPMGPEEEDSFSNAESYENADEELAQPVGRMMDF 471
                *************:**************:***:************ ****:***.* ***

CD19_HUMAN      LSPHGSAWDPSREATSLGSQSYEDMRGILYAAPQLRSIRGQPGPNHEEDADSYENMDNPD 538
CD19_MOUSE      LSPHGSAWDPSREASSLGSQSYEDMRGILYAAPQLHSIQS--GPSHEEDADSYENMDKSD 529
                **************:********************:**:.  **.************:.*

CD19_HUMAN      GPDPAWGGGGRMGTWSTR 556
CD19_MOUSE      DLEPAWEGEGHMGTWGTT 547
                . :*** * *:****.*
```

B

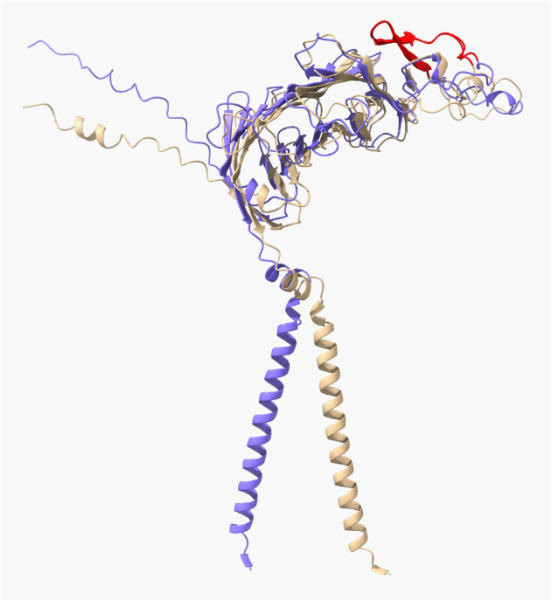

Figure S7. (A) Human and mouse CD19 multiple sequence alignment. CD19 protein sequences were obtained from Uniprot, and aligned using Clustal Omega with default settings. The region of the CD19 epitope (155-172 for CD19_HUMAN, 151-168 for CD19_MOUSE) is marked with 'E's above the sequence. **(B)** Human and mouse CD19 structure comparison. AlphaFold structure predictions for CD19 were obtained from Uniprot for human (tan) and mouse (blue). The epitope regions were aligned and colored red using ChimeraX. C-terminal polypeptides with poor AlphaFold prediction confidence scores were removed from the visualization (amino acids 331 to end for human, 329 to end for mouse). The structural similarity between the human and mouse CD19 proteins is high, especially in the area containing the epitope.